

EPA 600/R-04/120
September 2004

**Characteristics of Spilled Oils, Fuels, and Petroleum
Products: 3a. Simulation of Oil Spills and Dispersants
Under Conditions of Uncertainty**

by

James W. Weaver
Ecosystems Research Division
National Exposure Research Laboratory
Athens, Georgia 30605

National Exposure Research Laboratory
Office of Research and Development
U.S. Environmental Protection Agency
Research Triangle Park, NC 27711

Notice

The U.S. Environmental Protection Agency through its Office of Research and Development funded and managed the research described here. It has been subjected to the Agency's peer and administrative review and has been approved for publication as an EPA document. Mention of trade names or commercial products does not constitute endorsement or recommendation for use.

Foreword

The National Exposure Research Laboratory's Ecosystems Research Division (ERD) in Athens, Georgia, conducts research on organic and inorganic chemicals, greenhouse gas biogeochemical cycles, and land use perturbations that create direct and indirect, chemical and non-chemical stresses, exposures, and potential risks to humans and ecosystems. ERD develops, tests, applies and provides technical support for exposure and ecosystem response models used for assessing and managing risks to humans and ecosystems, within a watershed / regional context.

The Regulatory Support Branch (RSB) conducts problem-driven and applied research, develops technology tools, and provides technical support to customer Program and Regional Offices, States, Municipalities, and Tribes. Models are distributed and supported via the EPA Center for Exposure Assessment Modeling (CEAM) and through access to Internet tools (www.epa.gov/athens/onsite).

At the request of the US EPA Oil Program Center, ERD is developing an oil spill model that focuses on fate and transport of oil components under various response scenarios. This model includes various simulation options, including the use of chemical dispersing agents on oil slicks. The dispersant simulation is backed by empirical data on the effectiveness of dispersants and oil composition and properties. The model is offered as a tool for oil spill response and planning.

Rosemarie C. Russo, Ph.D.
Director
Ecosystems Research Division
Athens, Georgia

Oil Spill Report Series

A series of research reports is planned to present data and models for oil spill planning and response. To date, these include:

1. Oil Composition

Zhendi Wang, B.P. Hollebone, M. Fingas, B. Fieldhouse, L. Sigouin, M. Landriault, P. Smith, J. Noonan, and G. Thouin, 2003, Characteristics of Spilled Oils, Fuels, and Petroleum Products: 1. Composition and Properties of Selected Oils, United States Environmental Protection Agency, National Exposure Research Laboratory, EPA/600/R-03/072.

2. Dispersants

George Sorial, Subhashini Chandrasekar, James W. Weaver, 2004, Characteristics of Spilled Oils, Fuels, and Petroleum Products: 2a. Dispersant Effectiveness Data for a Suite of Environmental Conditions – The Effects of Temperature, Volatilization, and Energy, United States Environmental Protection Agency, National Exposure Research Laboratory, EPA/600/R-04/119.

3. Simulation Models

James W. Weaver, 2004, Characteristics of Spilled Oils, Fuels, and Petroleum Products: 3a. Simulation of Oil Spills and Dispersants Under Conditions of Uncertainty, United States Environmental Protection Agency, National Exposure Research Laboratory, EPA/600/R-04/120.

As more reports are added to the series, they may be found on EPA's web site at:
<http://www.epa.gov/athens/publications>.

Table of Contents

Notice	ii
Foreword	iii
Oil Spill Report Series	iv
List of Figures	vii
List of Tables	ix
1. Introduction	1
2. Implementation of the Model	2
The Four Applications Contained Within the ERO ³ S Frame	2
Oil Spreading	5
Floating Oil	7
Drift due to Winds and Currents	14
Mass Conservation	14
Prototype Equations for Non-Weathering Oils	16
Prototype Equations for Weathering Oils	17
Dispersal of Oil	18
Simulation of Oil Slicks	19
Uncertainty Analysis	20
Example	22
3. User's Guide	24
Applet versus Application	24
Software Requirements	24
Basic Interface Options	24
4. Conclusions	31
References	32
Appendices	34
Acronyms	34
Appendix: Latitude-Longitude Coordinates in ERO ³ S	35
Appendix: Model Development Within the MDP Model Development Platform	38

Procedural Outline for Creating MDP Applications	38
Directory and Package Structure	38
Appendix: Sorial et al. (2004) Dispersant Data	42
Appendix: Wang et al. (2003) Physical Properties and Chemical Composition of Alaska North Slope Crude Oil	55
Appendix: Wang et al, (2003) Physical Properties and Chemical Composition of South Louisiana	67
Appendix: Wang et al. (2003) Physical Properties and Chemical Composition of Fuel Oil No. 2/Diesel	79

List of Figures

Figure 1 ERO ³ S model selection screen.	2
Figure 2 Model implementation schematic showing user inputs and data, simulations, and the numerical solver. Dashed lines indicate inputs and solid lines represent results. The multiple circles or ellipses indicate separate options within the model	3
Figure 3 Computed radius (top) and height of an oil slick caused by the release of 11,000,000 gallons of Alaska North Slope crude oil. The formula used assumes an instantaneous release of the oil and is based on order of magnitude estimates.	10
Figure 4 Spatial concept used in the proposed model.	15
Figure 5 Relationship of uncertainty to model data availability.	21
Figure 6 Required options for use of ERO ³ S in Microsoft Internet Explorer.	25
Figure 7 Introductory ERO ³ S screen.	27
Figure 8 ERO ³ S identification screen.	28
Figure 9 ERO ³ S model selection screen.	28
Figure 10 ERO ³ S model screen example.	29
Figure 11 Illustration of latitude-longitude input for ship location and locations of shore line points.	35
Figure 12 Shorelines entered from lat-long data. The top shoreline's coordinates are shown in Figure . The ship itself is barely visible between the two shorelines, but can be seen in the close up at right.	35
Figure 13 Latitude-Longitude calculation in ERO ³ S.	36
Figure 14 Directory structure of the ERO ³ S MDP application. The two first level directories, ERO3S and modelsjavabase, are the locations that contain the code that is unique to ERO ³ S (ERO3S) and the MDP framework (modelsjavabase).	39
Figure 15 Directory structure of the Java MDP showing the required subdirectories: bak, classes, doc, package cache, and src. An src subdirectory is created by the MDP user for each new model and must contain additional subdirectories: gov, epa, first level name (here: modelsjavabase), and second level names (here: awtextend, doc, fw2, etc).	39
Figure 16 Estimated vs Measured % Dispersal of PBC with No Dispersant.	44
Figure 17 Estimated vs Measured % Dispersal of 2FO with No Dispersant.	44
Figure 18 Estimated vs Measured % Dispersal of SLC with No Dispersant.	44
Figure 19 Estimated vs Measured % Dispersal of PBC with Dispersant "A".	44
Figure 20 Estimated vs Measured % Dispersal of 2FO with Dispersant "A".	44
Figure 21 Estimated vs Measured % Dispersal of SLC with Dispersant "A".	44
Figure 22 Estimated vs Measured % Dispersal of BPC with Dispersant "B".	44
Figure 23 Estimated vs Measured % Dispersal of 2FO with Dispersant "B".	44
Figure 24 Estimated vs Measured % Dispersal of SLC with Dispersant "B".	44
Figure 25 Comparison of regression equations (curves) against measured Prudhoe Bay Crude/no dispersantefficiency.	46
Figure 26 Comparison of regression equations (curves) against measured Prudhoe Bay Crude/dispersant "A" efficiency.	46

Figure 27 Comparison of regression equations (curves) against measured Prudhoe Bay Crude/dispersant “B” efficiency.	47
Figure 28 Comparison of regression equations (curves) against measured South Louisiana Crude/No Dispersant efficiency.	48
Figure 29 Comparison of regression equations (curves) against measured South Louisiana Crude/Dispersant “A” efficiency.	49
Figure 30 Comparison of regression equations (curves) against measured South Louisiana Crude/Dispersant “B” efficiency.	50
Figure 31 Comparison of regression equations (curves) against measured No. 2 Fuel Oil/No Dispersant efficiency.	51
Figure 32 Comparison of regression equations (curves) against measured No. 2 Fuel Oil/Dispersant “A” efficiency.	52
Figure 33 Comparison of regression equations (curves) against measured No. 2 Fuel Oil/Dispersant “B” efficiency.	53

List of Tables

Table 1 Example values of surface tension, interfacial tension and spreading forces for a suite of oils (Environment Canada, 1999).	6
Table 2 Density and viscosity of selected oils (Environment Canada, 1999, ^(a) 2004).	12
Table 3 Variable parameters for uncertainty analysis example.	22
Table 4 Example uncertainty analysis results.	23
Table 5 Coefficients of Regression Equations with Terms Determined by Step-Wise Linear Regression	43

1. Introduction

The EPA Research Object-Oriented Oil Spill (ERO³S) model has been developed as a Federal-employee lead effort to develop a model that

1. Is in the public domain,
2. Is developed and understood by EPA employees,
3. Where EPA's commitment transcends limited-term contracting/grant/cooperative-agreement/Interagency Agreement (IGA) vehicles,
4. can be modified to meet needs identified by EPA Regional Offices, and
5. that includes state-of-the-art concepts in modeling -- note especially the uncertainty analysis capability and implementation in an object-oriented language.

The model was designed using concepts of object-oriented programming. Although this may seem to be a programming detail, object-oriented software design is viewed as enhancing maintainability and re-use of computer code. The approach taken for ERO³S naturally has these features, but two others are important: 1) by implementing the model in Java, a version of the code can run as a client-side applet from a web page and 2) the oil spill problem naturally aligns with object-oriented programming.

The last point bears amplification. Oil spills are commonly observed to be “patchy.” Oil does not spread as a uniform pancake across the surface of the water. It is broken, rather, into separate bodies of oil. These, however, share common characteristics: they are all composed of oil, they all spread according to the same basic physics, they weather according to the same physio-chemical processes. For example, the differences between patches depend more on factors of time-in-water, current variations or shorelines encountered, and direct application of a dispersant to part of the whole spill. From these attributes, common behavior can be programmed for a single generic oil slick and individual differences among slicks essentially become differences in their data. Thus transport of a patchy oil slick aligns closely with an object-oriented approach, more so than many other problems.

2. Implementation of the Model

The EPA Research Object-Oriented Oil Spill (ERO³S) was designed using object-oriented programming concepts. Hence the inclusion of the phrase “Object-Oriented” in the title. Use of common components (classes) is the software implementation feature that allows the parts of each model to be recombined and reused in the more complex applications. These same ideas are used in the ERO³S frame to provide components of the graphical user interface (GUI). These features are mostly invisible to the model users, but the repetition of model input or output screens is evidence of component reuse.

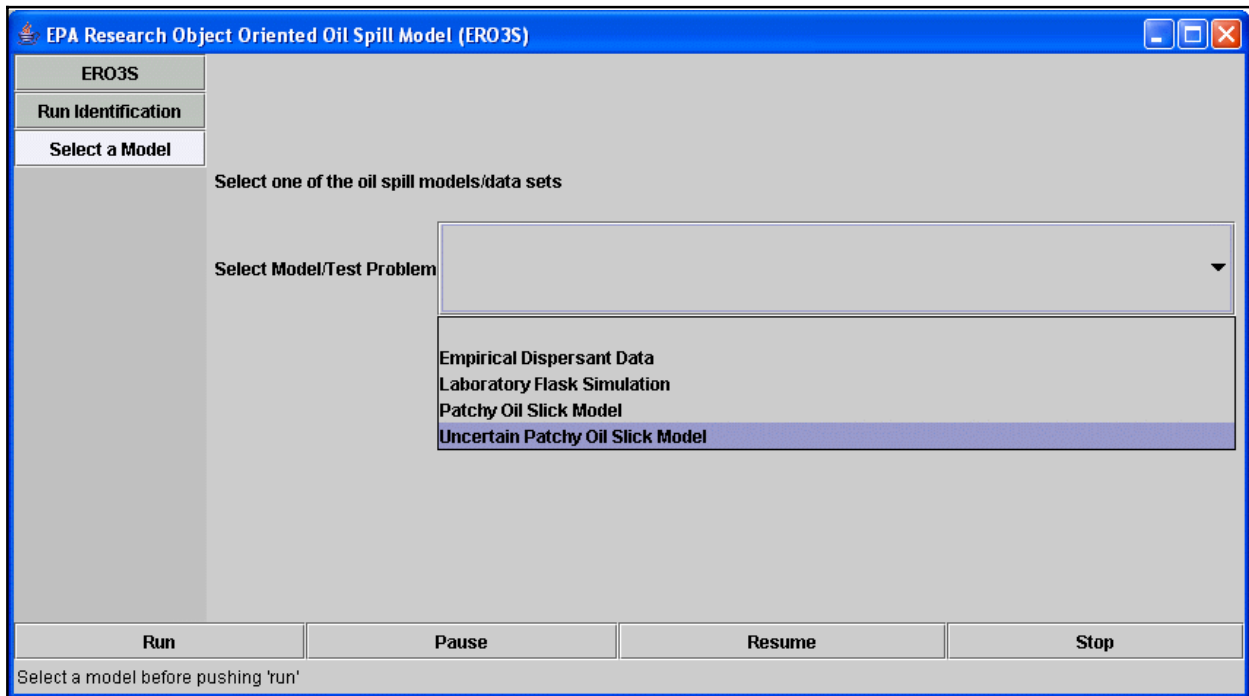


Figure 1 ERO³S model selection screen.

The Four Applications Contained Within the ERO³S Frame

Figure 1 indicates four choices of models within the ERO³S frame. These present various oil spill research results and increase in complexity following the sequence:

1. **Empirical Dispersant Data.** Data from laboratory experiments on dispersion of oil in the US EPA baffled flask test (BFT) are presented in a graphical form.¹
2. **Laboratory Flask Simulation.** A simulation of the baffled flask test data is performed as if dispersant is added at specified times during the simulation. Data on oil composition and weathering are also used in the simulation.
3. **Patchy Oil Slick Model.** Because most observers note that oil slicks are patchy or broken up into small bodies of oil, an oil slick model is implemented that simulates spreading of small patches of oil that compose the entire oil slick. These sub-slicks are independently spread, weathered, transported and dispersed with dispersant. Components from each of the prior applications and a model of spreading and transport of a single slick are used in the patchy oil slick model.
4. **Uncertain Patchy Oil Slick Model.** All model input parameters have associated levels of uncertainty; some are not measured or even measurable. For example, the release rate or volume is seldom known, the oil composition varies, the wind and current magnitude and directions change or are only approximately known. Consequently, a modeling analysis should include evaluation of uncertainties. In ERO³S, uncertainty is included in the calculation by a simple method: ranges of several input parameters are selected, then the model is run for all combinations of these inputs. Extreme values of a set of model outputs are generated and given as outputs. This approach gives the model user an indication of the uncertainty in model results, given the specified ranges of model inputs.

¹EPA currently requires results from a swirling flask test for placement of products on the Subpart J products list. The baffled flask test has been proposed as a better alternative to the swirling flask test.

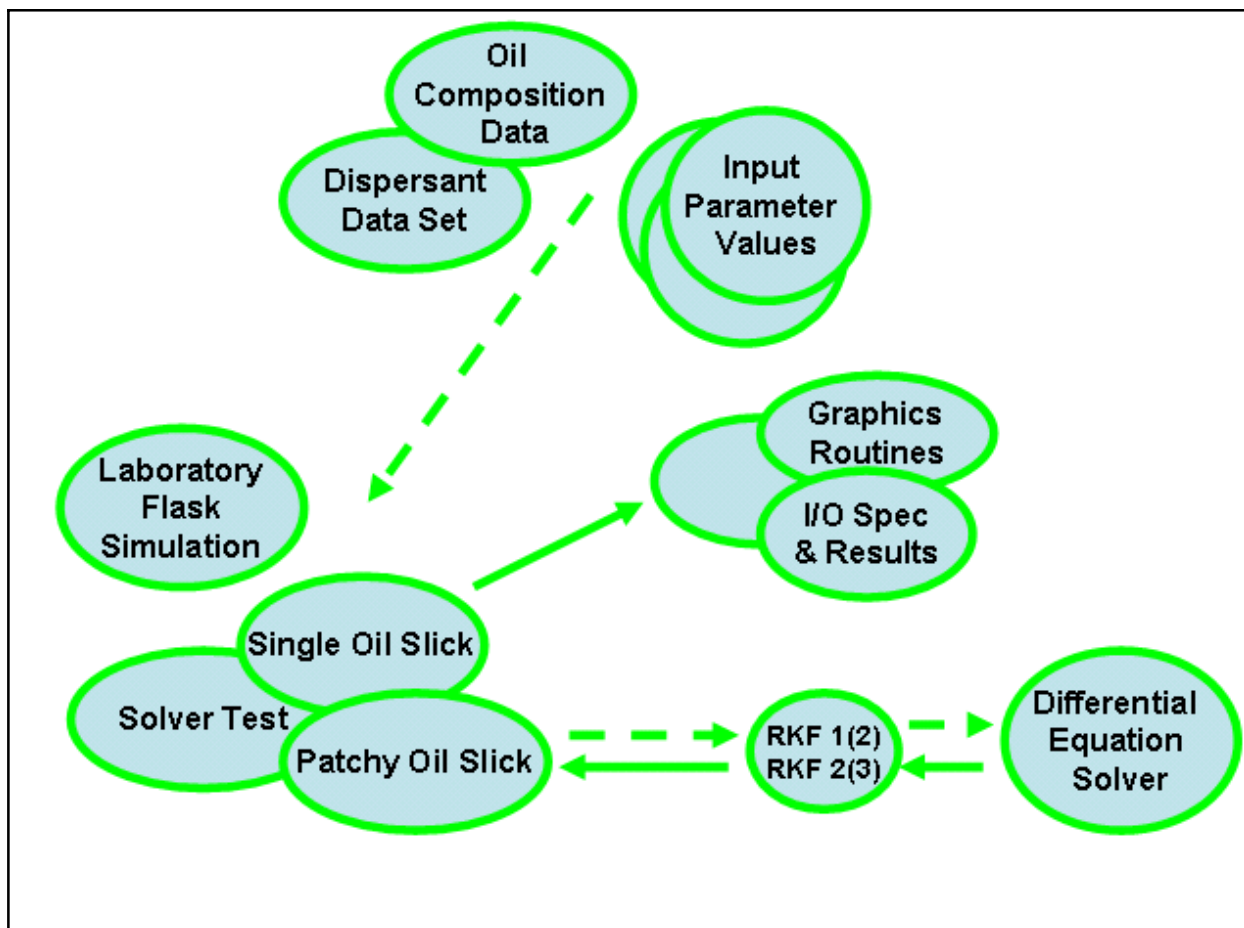


Figure 2 Model implementation schematic showing user inputs and data, simulations, and the numerical solver. Dashed lines indicate inputs and solid lines represent results. The multiple circles or ellipses indicate separate options within the model.

An outline of the model structure is contained in an Appendix that describes the Model Development Platform (MDP) that was created for this work. MDP contains functions for all the required elements of the model: the user interface, graphics, numerical input/output, numerical solvers, and utility routines to execute the model. The model itself is created as a specialized subset of the MDP, which is combined with the generic capability to become the model (i.e., ERO³S).

Figure 2 illustrates the internal structure of the MDP that allows the four options described above. Multiple circles or ellipses on the figure indicate separate choices or options that are available under certain circumstances. The dashed lines indicate internal passage of data. User input is collected on input screens (Input Parameter Values) and combined with built-in data on oil composition and dispersant effectiveness. These are passed to one of several models: Single Oil Slick, Patchy Oil Slick or Laboratory Flask Simulation. Of these, the first two use an ordinary differential equation solver to generate the solution. The Laboratory Flask Simulation,

being a set of simple calculations requires no numerical solver. The solver uses an explicit Runge-Kutta method. The specific method is selectable from a number of choices that include embedded time stepping control, implemented through Runge-Kutta Fehlberg (RKF) algorithms (Fehlberg, 1969). The coefficients are represented by the ellipse indicating RKF1(2) and RKF2(3) methods. These methods allow for automated time-step controlling through the embedding of a more accurate higher-order method within a lower-order method. RKF1(2), for example, uses a first order method to generate its solution and a second order method to estimate error and thus modify time steps, if necessary (Fehlberg, 1969). Methods of up to seventh order are available (RKF7(8)) in the framework, but rarely necessary (Hairer et al, 1993). These procedures allow the model to increase or decrease the time step as needed to maintain accuracy of the results.

The structure also allows for time step changes that are required by the characteristics of the problem. For example, the model should have a time step that begins at the time(s) that dispersant is applied. Such a happening in the model is called a “solution” event and the model time steps are adjusted so that these occur at the beginning/ending of a time step.

Oil Spreading

In any of the oil spreading applications in ERO³S, the same basic physics apply; either if the slick is composed of a single pancake or a set of individual slicks. The following section describes the spreading algorithms.

The tendency for oil to spread is given by (e.g., Canevari, 1969)

$$F = \sigma_w - \sigma_o - \sigma_{ow} \quad (1)$$

where F is the spreading force, σ_w is the surface tension of water, σ_o is the surface tension of oil and σ_{ow} is the oil/water interfacial tension. Table 1 lists surface and interfacial tensions for a number of crude oils and petroleum products. The estimated spreading force for salt and fresh water is given in the last two columns (assuming that the surface tension of water is 65 dyne/cm). Of all the oils listed, only Jet A-1 has a negative spreading force. The surface and interfacial tension data suggest that all other of these oils tend to spread over the surface of water, at least as long as the surface and interfacial tensions are unchanged by weathering.

Observation of oil spills provide insight on the minimum oil thickness that may occur. For example, the US Coast Guard Fact Sheet on Small Diesel Spills (500-5000 gallons) states that heavy diesel sheens contain about 1000 gallons per square nautical mile of surface and that silver sheens contain about 75 gallons per square nautical mile. These observations imply thicknesses of 1.18×10^{-2} mm down to 8.91×10^{-4} mm. Reports on slick thicknesses suggest that a bounding thickness is reached that may be due to surface tension changes (Fay, 1969).

The model needs to account for the thickness of floating oil bodies, because at a minimum the volume and thickness are prime determinants of the area of contact between the slick and the water, and between the slick and the air. Both of these areas of contact are important for determining the mass transfer rate of chemicals into these media. The observations on lens thickness and surface tensions suggest three interrelated components of spreading:

- transient, short-lived, thick oil layers
- surface tension driven spreading of thin layers
- weathering induced changes in surface and interfacial tension

The following section provides a simplified methodology for including the first two of these components. Because of the complexity of interactions during weathering, the effect of weathering on surface and interfacial tension is included empirically through data collected on oil composition and properties (Wang et al., 2002).

Fuel or Crude Oil	Surface Tension dyne/cm	Oil/Salt Water Interfacial Tension dyne/cm	Oil/Fresh Water Interfacial Tension dyne/cm	Spreading Force dyne/cm	
				Salt Water	Fresh Water
Santa Clara	28.7	23.3	25.7	13.1	10.6
Prudhoe Bay	28.3	9.7	16.9	27.0	19.8
Arabian Medium	27	20.8	21.7	17.2	16.3
Alaska North Slope	28.1	27.4	29.4	9.5	7.5
Kuwait	27.8	22.9	28.6	14.3	8.6
Iranian Heavy	26.1	22.5	22.5	16.4	16.4
Alberta Sweet Blend	25.6	8.4	21.5	31.0	17.9
Louisiana	25.9	19.6	21.1	19.5	18.0
West Texas Intermediate	26.6	18.9	19.1	19.5	19.3
Barrow Island	26.2	15.9	18.1	22.9	20.7
Diesel Fuel	26.5	28	29.4	10.5	9.1
Aviation Gas 100	20	42.2	42.2	2.8	2.8
Jet B	23	10.8	12.4	31.2	29.5
JP-4	22.8	17	36	25.2	6.2
Jet A-1	26	38.4	40.4	0.6	-1.4
Leaded Gasoline	19.8	18.6	18	26.6	27.2

Table 1 Example values of surface tension, interfacial tension and spreading forces for a suite of oils (Environment Canada, 1999).

Floating Oil

Mass and momentum conservation for the oil as a separate phase determines how oil floats on the water surface. Three stages have been identified in the spreading of an oil slick (Fay, 1969, Houtt, 1972, Buckmaster, 1973, U.S. Coast Guard, 1994). In the first stage gravity and inertial forces control the spreading of oil across the surface. In the second stage, the inertial forces become negligible in comparison with viscous drag across the surface. In the third stage interfacial forces become dominant and provide the driving force to propel spreading. Thus, at equilibrium the floating oil could spread across the surface or it could form a lens. The occurrence of these two types of behaviors depends on the relative magnitudes of the surface and interfacial tension forces. Data presented in the table above show that for almost all of the oils in

fresh and salt waters, the final stage would be characterized by spreading across the water, because the values of the spreading force, F , are positive. This is, of course, true if the values in the table well represent these oils and if weathering in stages 1 and 2 does not affect the surface and interfacial tension values.

The most commonly used simple formulations for oil spreading were developed by Fay (1969). The relations derived by Fay were intended to “estimate the order of magnitude of the rate of spread of an oil slick on the surface of still water, i.e., water which is free of motions induced by wind, wave, tidal currents.” The analysis can clearly be seen to be only based on order of magnitude estimates by Fay’s omission of π and other constants in formulas for volume and area (equation 1 and 3 of Fay, 1969). Fay’s discussion indicates his belief that gravity, inertia, viscous and surface tension forces are dominant in causing spreading, even when subject to winds, waves, and currents. Hoult (1972) describes a commonly held assumption that the spread of an oil slick is composed of two parts, the first driven by winds and currents, and the second due to the innate tendency of the oil to spread on even a calm surface. These two physical phenomena are built into the ERO³S model. The necessity of this approach is fairly obvious, as oil spilled into a calm environment would spread simply because of its innate tendencies, while oil spilled into rapidly flowing water would spread both to its spreading tendency and because of the action of wind and waves. The point being that the motion of the oil may be dominated by one or the other of these two phenomena depending upon the situation.

Following Fay’s analysis for spreading on calm seas, the gravity force is proportional to the volume of the oil, V ,

$$V = \frac{\pi}{4}d^2h \propto d^2h \quad (2)$$

where d is the oil slick diameter and h is the slick height. Both d and h are assumed to vary with time in this analysis. The gravity force per unit volume of oil is proportional to

$$\Delta\rho gV / d^3 \quad (3)$$

where $\Delta\rho$ is the difference in density between water and oil, and g is the acceleration of gravity. The net effect of surface tension is to spread the oils listed in Table 1. The magnitude of the surface tension force is given by

$$\frac{\sigma d}{V} \quad (4)$$

where σ is the net surface tension. Comparing the gravity and surface tension force expressions shows that for a fixed volume, V , the magnitude of the gravity force will decrease with time as

the diameter, d , increases; and that the magnitude of the surface tension force will increase with diameter (time). Equating the two forces gives a critical diameter beyond which spreading is dominated by surface tension. The critical diameter, d_c , is proportional to

$$d = \sqrt[4]{\frac{\Delta\rho g V^2}{\sigma}} \quad (5)$$

Inertial and viscous forces act to retard the spreading of the oil. The inertial force is the product of density and acceleration

$$\rho \frac{d}{t^2} \quad (6)$$

Viscous forces are proportional to

$$\frac{\rho v^{1/2} d^3}{V t^{3/2}} \quad (7)$$

The ratio of viscous to inertia forces is proportional to

$$d^2 t^{1/2} \quad (8)$$

showing that inertial forces are dominant at early times (because at early times t , and thus $t^{1/2}$ is small, meaning that inertial forces are much greater than viscous forces).

Extending Fay's analysis by equating all four forces so that gravity and surface tension are balanced by viscous and inertial resistance to flow gives an equation for the slick radius at all times:

$$\frac{\Delta\rho g V}{d^3} + d \left(\frac{\sigma}{V} - \frac{\rho}{t^2} \right) - \frac{\rho v^{1/2} d^3}{V t^{3/2}} = 0 \quad (9)$$

The surface tension term may be positive or negative, depending on the magnitude of the spreading force, F . Thus the equation allows for surface tension to act against spreading. This equation must be solved iteratively because it is nonlinear, but it combines all the mechanisms used in Fay's analysis. By doing so, the original assumption that the three stages are driven by mutually exclusive force pairs (gravity-inertia, gravity-viscous, and surface tension-viscous) is relaxed. In Fay's analysis transition times would be calculated and an equation is used to corresponds to a the appropriate force-pair is used. In the ERO³S approach the extended Fay

equation applies at all times and the relative magnitudes of each term determine which process is dominant.

Figure 1 shows the computed results for a spill similar to the Exxon Valdez. The oil was assumed to have the same properties as the Alaska North Slope Crude described in Tables 1 and 2; and the volume was taken as 11,000,000 gallons. Data from spills, however, is needed to estimate proportionality constants that have been ignored in the Fay analysis. The radius estimate also shows the effects of assuming an instantaneous release—all eleven million gallons were released instantaneously. Figure 3 shows that the initial increase in radius is very rapid, followed by a continuing increase over time. The slick height decreases very rapidly to a thickness of 10 cm and decreases to less than 0.1 mm before the end of one year. Despite its limitations, this model shows that the lens increases in radius and decreases in thickness rapidly, in agreement with generalized observations.

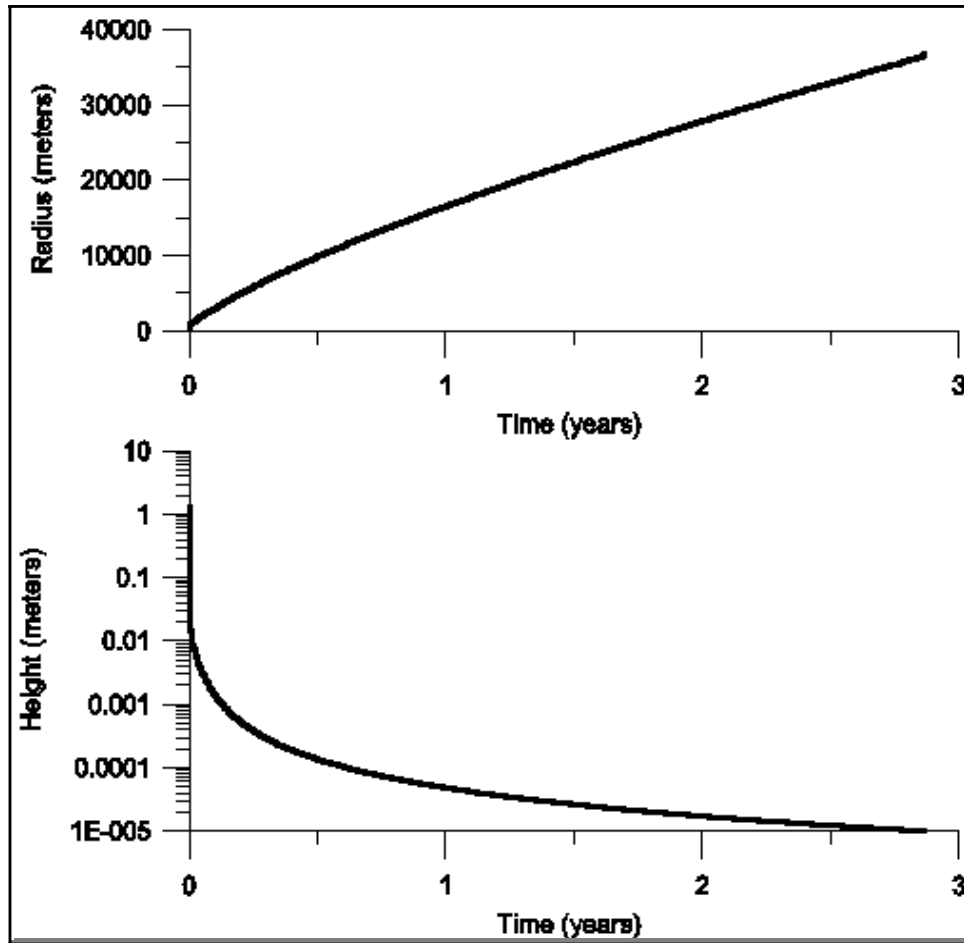


Figure 3 Computed radius (top) and height of an oil slick caused by the release of 11,000,000 gallons of Alaska North Slope crude oil. The formula used assumes an instantaneous release of the oil and is based on order of magnitude estimates.

Fuel or Crude Oil	Density		Dynamic Viscosity	
	g/cm ³		cP (or mPa s)	
	0 °C	15 °C	0 °C	15 °C
Santa Clara	0.93	0.92	1278	304
Prudhoe Bay	0.92	0.91	577	68
Arabian Medium	0.89	0.88	59	29
Alaska North Slope	0.90	0.89	^(a) 23	^(a) 12
Kuwait	0.88	0.87	90	22
Iranian Heavy	0.89	0.88	43	20
Alberta Sweet Blend	0.85	0.84	47	9
Louisiana	0.86	0.85	15	8
West Texas Intermediate	0.85	0.83	15	7
Barrow Island	0.85	0.84	4	2
Diesel Fuel	0.84	0.84	4	2
Aviation Gas 100	0.73	0.72	1	1
Jet B	0.77	0.76	1	1
JP-4	0.77	0.83	1	1
Jet A-1	0.82	0.80	2	1
Leaded Gasoline	0.75	0.74	0.8	0.6

Table 2 Density and viscosity of selected oils (Environment Canada, 1999, ^(a)2004).

Fay's analysis also includes the release of oil at a fixed flow rate, V_f , into a flowing current of velocity, u . The formula analogous to that given above, combining gravity, inertial, viscous, and surface tension forces is

$$\frac{\Delta\rho g V_f}{d^2 u} + d \left(\frac{u}{V_f} - \frac{\rho u^2}{x^2} \right) - \frac{\rho \nu^{1/2} d^2 u^{5/2}}{V_f x^{3/2}} = 0 \quad (10)$$

where x is the distance down stream from the source.

The coefficients which make the preceding relationships precise can be determined either by experiment or by theoretical analysis. As an example of the latter, the Buckmaster (1973) analysis begins with the governing equations for the stage 2 problem—gravity/viscous flow. The governing equations for the oil are the mass and momentum conservation equations, given by

$$-\frac{\nu}{g\Delta\rho}\frac{\partial u}{\partial y}(x,0;t) + h\frac{\partial h}{\partial t} = 0 \quad (11)$$

and

$$\frac{\partial h}{\partial t} + \frac{\partial(qh)}{\partial x} = 0 \quad (12)$$

where $h(x,t)$ is the thickness of the slick, $q(x,t)$ the oil velocity, g is the acceleration due to gravity, $\Delta\rho$ is the fractional density difference between the oil and water, ν is the kinematic viscosity of the oil.

For the water

$$\frac{\partial u}{\partial t} + u\frac{\partial u}{\partial x} + v\frac{\partial u}{\partial y} = \nu\frac{\partial^2 u}{\partial y^2} \quad (13)$$

and

$$\frac{\partial u}{\partial x} + \frac{\partial v}{\partial y} = 0 \quad (14)$$

Buckmaster outlines a solution approach for computing the size and shape of the lens as a function of time. Ultimately Buckmaster derived from this theory an expression for the radius of slick, R , as

$$R(t) = 1.76(g\Delta\rho)^{0.25} V^{0.3333} \nu^{-0.125} t^{0.375} \quad (15)$$

where V is the volume of the slick. The leading coefficient (1.76) differed from a previously observed empirical value of 1.5 (Hoult, 1972) by 15%.

Drift due to Winds and Currents

In Hoult's conceptualization, the effects of winds and currents can be separated from the spreading discussed above. In essence, the two sets of phenomena are superimposed upon each other as the processes which cause spreading in calm seas are viewed as inexorable processes also occurring when currents drive flow in a certain direction. Hoult (1972) estimated drift due to the wind by equating shear stresses in the water and air and derived the result that

$$U_w \cong 0.03U_a \quad (16)$$

where U_w is the wind-induced drift velocity and U_a is the wind speed. The coefficient 0.03 results from the differing densities of air and water. Further, the movement of the center of mass, X , of the oil slick is given by

$$\frac{dx}{dt} = U_c + 0.03U_a \quad (17)$$

where U_c is the velocity of the current itself. The importance of the last equation is that it provides a simplified means of accounting movement of the slick caused by wind and currents.

Mass Conservation

The implementation of ERO³S is based upon the equations given in the following summary. The two fundamental equations of fluid mechanics for incompressible flows are conservation of mass and conservation of momentum. Conservation of mass is invoked in the proposed model by

$$\sum \frac{\partial M_i}{\partial t} + \nabla \cdot J_{m_i} = r_i \quad (18)$$

Conservation of momentum is included indirectly by using the extended Fay equation given above

$$\frac{\Delta \rho g V}{d^3} + d \left(\frac{\sigma}{V} - \frac{\rho}{t^2} \right) - \frac{\rho v^{1/2} d^3}{V t^{3/2}} = 0 \quad (19)$$

The relationship between the volume, V , and characteristic planar dimension, d , is assumed to be governed by a circle in the absence of winds and currents (Figure 4). Since winds and currents will almost always be important for oil spills, this spatial relationship will be changed to an

ellipse as the slick evolves (i.e., the circle is only an initial condition for the ellipse, which is anticipated to be used in virtually every case). An ellipse has the form

$$\frac{x^2}{a^2} + \frac{y^2}{b^2} = 1 \tag{20}$$

where the coefficients a, and b describe the properties of the ellipse (in the same way that the single coefficient, the radius, completely describes the properties of a circle). A circle is centered in space at a single point, the center; while an ellipse is characterized by two foci. For the oil spill problem, the release of oil will be assumed to occur at one focus of the ellipse. As long as oil is being released the location of the release focus will remain fixed. Once the release ends, the entire slick will be allowed to drift with wind and currents. Elongation and drift will be calculated from the relationship

$$l = \int_{t=0}^{t < t_e} (U_c + 0.03U_a) dt \tag{21}$$

where l represents the length of the ellipse. Note that the initial length is equal to zero. As the length of the ellipse increases with time, the volume of the slick is conserved and the shape is governed by the extended Fay equation. The result will be that the slick increases in length and the distance between the foci of the ellipse increases. Thus the shape of the lens is determined by the effects of wind and current according to the relationship for spreading that relates gravity, inertial, viscous and surface tension forces. Hoult's conception that the spreading occurs independently of drift is incorporated into this proposed approach.

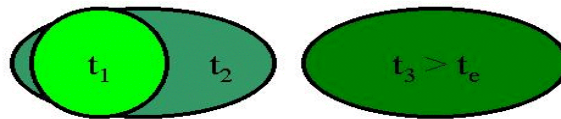


Figure 4 Spatial concept used in the proposed model. At time of t_1 there has been no impact of wind nor currents on the soil slick and its shape is circular. At t_2 the slick has elongated because of wind and/or waves. At time t_3 the release has ended and the slick is drifting away from the source. For most cases of interest the circular shape of t_1 is expected only to be an initial condition of the model and elongation is expected from the start.

After the release ends the slick may drift away from the source. Thus the position of the center of mass of the slick is given by

$$x = x_e + \int_{t_e}^t (U_c + 0.03U_a) dt \quad (22)$$

where x is the location of the center of mass of the slick and x_e is the center of mass position at the end of the release.

Prototype Equations for Non-Weathering Oils

The prototype equations for the mathematical system are

$$\frac{DV}{Dt} = R \quad (23)$$

where V is the oil volume and R is the rate of release of the oil. By treating the release as an ordinary differential equation, the restrictions of Fay's analysis are relaxed: the release does not have to be instantaneous nor continuous (equation 10). Since the ordinary differential equation solver was designed to use automated time step control based upon Fehlberg's method embedding approach (Hairer, 1993), the solver can be used also to step to specified times in the solution. These are called solution events, and are used extensively in controlling the execution of the ERO³S model. The oil spill ending time is the first of the important solution events included in the model

The extended Fay equation (9) has the general form:

$$F(V(t), d(t), t; \Delta\rho, \rho, \sigma, \nu, g) = 0 \quad (24)$$

where the volume, V , and characteristic size, d , are functions of time. All quantities to the right of the semicolon are assumed to be constants, when weathering is ignored. Therefore application of the implicit function theorem of calculus leads to

$$\frac{DF}{Dt} = \frac{\partial f}{\partial t} + \frac{\partial f}{\partial V} \frac{dV}{dt} + \frac{\partial f}{\partial d} \frac{dd}{dt} = 0 \quad (25)$$

and

$$\frac{dd}{dt} = \frac{-\frac{\partial f}{\partial t} - \frac{\partial f}{\partial V} \frac{dV}{dt}}{\frac{\partial f}{\partial d}} \quad (26)$$

The two differential equations can be solve numerically for V(t) and d(t). The size of the lens then determined from

$$l = 2a \Rightarrow \frac{dl}{dt} = 2 \frac{da}{dt} = (U_c + 0.03U_a) \quad (27)$$

and

$$d = \frac{1}{2}(a + b) \quad (28)$$

The lens height, h, is determined from the ellipse volume $V = h \pi a b$.

Prototype Equations for Weathering Oils

The prototype equations are extended to include the effects of weathering. The prototype equations for the mathematical system become

$$\frac{DV}{Dt} = R \quad (29)$$

where V is the oil volume and R is the rate of release of the oil.

The extended Fay equation (9) has the general form, if weathering effects on the oil physical properties are included:

$$F(V(t), d(t), \Delta\rho(t), \rho(t), \sigma(t), \nu(t), t; g) = 0 \quad (30)$$

where the volume, dimensions and physical properties (density, viscosity, surface tension) are now all potentially functions of time. Therefore

$$\frac{DF}{Dt} = \frac{\partial f}{\partial t} + \frac{\partial f}{\partial V} \frac{dV}{dt} + \frac{\partial f}{\partial d} \frac{dd}{dt} + \frac{\partial f}{\partial \Delta\rho} \frac{d\Delta\rho}{dt} + \frac{\partial f}{\partial \rho} \frac{d\rho}{dt} + \frac{\partial f}{\partial \sigma} \frac{d\sigma}{dt} + \frac{\partial f}{\partial \mu} \frac{d\mu}{dt} = 0 \quad (31)$$

and

$$\frac{dd}{dt} = \frac{-\frac{\partial f}{\partial t} - \frac{\partial f}{\partial V} \frac{dV}{dt} - \frac{\partial f}{\partial \Delta \rho} \frac{d\Delta \rho}{dt} - \frac{\partial f}{\partial \rho} \frac{d\rho}{dt} - \frac{\partial f}{\partial \sigma} \frac{d\sigma}{dt} - \frac{\partial f}{\partial \mu} \frac{d\mu}{dt}}{\frac{\partial f}{\partial d}} \quad (32)$$

Again the two differential equations can be solve numerically for V(t) and d(t). The rate of change of the function f with respect to each physical parameter can be determined analytically from equation 9. The change of each physical parameter with time is determined from the cumulative weathering of the oil and empirical data on the oil properties and the derivative is approximated by a simple differencing formula.

Dispersal of Oil

The amount of oil dispersed, V_{od} , is estimated from

$$V_{od} = d_{or} V_{d(actual)} E(t,w,e) \quad (33)$$

where $V_{d(actual)}$ is the volume of dispersant used to disperse the slick at a dispersant/oil ratio d_{or} , and $E(t,w,e)$ is the dispersant efficiency as a function of temperature, t, weathering, w, and sea state, e. The dispersal efficiency, $E(t,w,e)$, is assumed to follow laboratory data collected from the U.S. EPA baffled flask test.

The dispersant is applied at pre-selected times during the simulation. At these times a volume of dispersant, V_d , is assumed to be available to disperse the slick. The dispersant volume scheduled for application may or may not match the amount needed to disperse the slick. The amount of dispersant actually used is the smaller of

$$V_{d(actual)} = V_{os} / d_{or} \quad (34)$$

or

$$V_{d(actual)} = V_d d_{or} \quad (35)$$

where V_{os} is the volume of oil contained in the slick. Equation 34 is used when there is ample dispersant for the amount of oil present; equation 35 is used otherwise.

The dispersal efficiency is determined from the empirical data of Wang et al. (2003) and Sorial et al. (2004). Wang et al. (2003) developed a suite of compositional and property data for a suite of oils. Included are data for an Alaska North Slope crude, a South Louisiana crude and No. 2 Fuel oil which appear in appendices. For each oil an empirical expression was determined for volatilization. The best fit to

$$\% E = (A + B) \ln t \quad (36)$$

or

$$\% E = (A + B) \sqrt{t} \quad (37)$$

where %E is the weight percent evaporated, T is the sea surface temperature (°C), t is the time in minutes, and A and B are coefficients that are determined experimentally, is used to approximate volatilization and consequent property changes of the oils. As appear in the appendices, the density, viscosity, surface and interfacial tensions vary with volatilization and data on these are used in ERO³S to track changes in these properties. The data sets also include compositional and emulsification data which can also be driven by volatilization of the oil. Volatilization then provides a “master variable” that is used to access a variety of other empirical data on these oils.

Once the amount of weathering has been determined, the data developed by Sorial et al (2004) are used with the temperature, energy level and dispersant type to determine the amount of dispersal of the oil that is possible (E(t,w,e) in equation 33). The Sorial data set contain data for various volatilization weatherings (up to the maximum possible for the oil), temperatures from 5 °C to 35 °C, speeds of rotation of the test apparatus that represent varying energy levels, and three dispersant treatments. These treatments are two dispersants code-named “A” and “B” and a set of data collected with no dispersant. These served both as controls for experiments with “A” and “B,” as well as providing data on natural dispersion of these oils.

After the oil is dispersed the slick dimension and total volume of floating and dispersed oil are recalculated based upon the new volume of the slick or each slick if the patchy oil slick model is used.

Simulation of Oil Slicks

Spreading and dispersal of oil slicks are two basic functions of the code. As noted by Hoult (1972), transport with wind and waves are of equal importance. These are implemented in the most flexible fashion in the patchy oil slick model and the subsequent discussion will focus on this model.

The overall mass balance is tracked by solving equation 23, which has the effect of simply adding up the mass of oil released². The mass is divided in the model, however, into

²Even though this calculation could be performed simply as a summation of the oil released, including it as an ordinary differential equation to solve forces the mass balance

separate oil slicks which represent patches of the complete slick. This procedure provides the flexibility to allow:

- volatilization to change the composition of parts of the slick depending upon their time-in-water,
- different portions of the slick to move in response to variation in current or wind, and
- the dispersal efficiency to vary both due to oil properties and the amount of dispersant available.

The procedure that is followed for each individual patch is as follows:

- the beginning and ending times of its release are determined,
- the release rate is set,
- the initial composition is set, and
- a direction of transport and release point are assigned.

One thousand of these individual slicks are used to compose the entire oil slick. The spreading of each slick is determined from one run of the single slick model. A single slick model is executed for the oil, climatic conditions and release rate of the entire slick. This model is run until a minimum thickness is achieved and the results are saved for use in the individual slicks of the patchy oil slick model. The ERO³S model then tracks each of these slicks, determines their changes in composition and oil properties, and when the time comes for dispersant application, disperses a fraction of their oil in accordance with the properties of the oil and dispersant subject to the limitation of dispersant availability.

Uncertainty Analysis

Models, though, are commonly viewed as useful tools for understanding contaminant transport (Oreskes et al., 1994) and determining future risk (ASTM, 1995). The degree of predictive capability of most transport models has, in fact, not been established. This follows from the models' reliance on unmeasured input parameters and calibration to specific incidents. Given that the values of all the parameters and the forcing function were known, and that the assumptions behind the model were exactly met, the model equations could be solved for the required outputs. In the real world, however, the values are not exactly known and because response is the priority at oil spills, data collection for modeling or other purposes is generally not undertaken. Time is also critical, as decisions must be made quickly to minimize environmental impacts. This constraint alone imposes severe limitations on data collection. Simple examples of limited knowledge are the release rate or volume, composition and properties of the oil and climatic conditions controlling transport.

calculation to always be in synch with all other equations solved.

Thus, models are more likely to provide a framework for understanding transport than for predicting future exposure and risk. At an oil spill rapid response is required and sufficient data is not likely to be collected for calibrating a model. How then should models be used in situations where they can not or will not be calibrated? What are the plausible ranges of output given uncertainty in inputs? Can worst case parameter sets be selected that always provide a bound on plausible outcomes?

Figure 5 shows a conceptual relationship between uncertainty and data availability. With small amounts of either measured input data or calibration data, the resulting model uncertainty is high. Models may still be useful in these cases, but their uncertainty should be quantified so that their results are not taken falsely as inerrant.

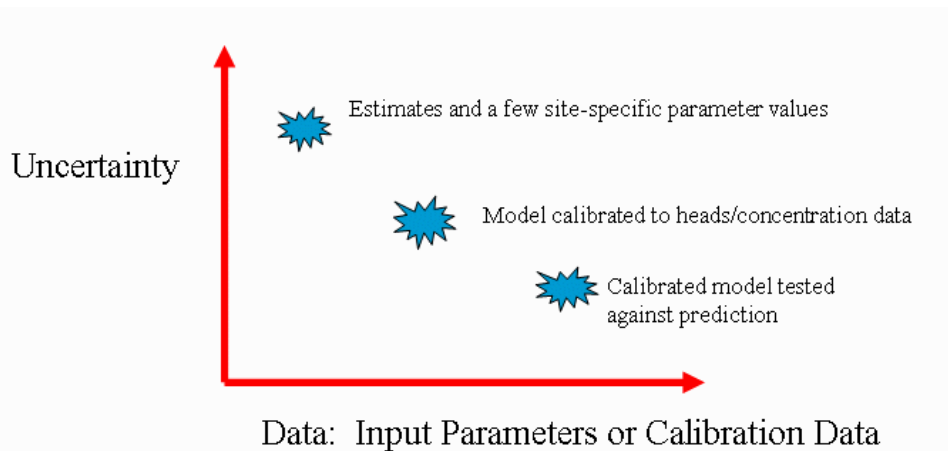


Figure 5 Relationship of uncertainty to model data availability.

Approach

Several approaches to uncertainty analysis have been developed. Generally these require knowledge of parameter values and their statistical distributions including correlations between individual parameters. For the purpose of the ERO³S code it is presumed that data collection is not sufficiently detailed to determine values for some of the parameters, let alone their statistical distributions and correlations.

A widely-used alternative is to assume knowledge of the statistical properties by using scientific literature values as substitutes. These approaches allow assignment of probabilities to the various outcomes, but suffers from obvious lack of incident-specificity. Where results depend strongly on assumed distributions, it is not possible to determine how much error is introduced into the results from the distributions. Alternatively, if it is assumed only that plausible ranges of input parameters are known, similar outcomes can be determined, but probabilities cannot be assigned. Because of presumed lack of knowledge of certain parameters and their underlying probability distributions, a method based on ranges of inputs was developed.

In the ERO³S code, bounding values of selected parameters are input. The minimum and maximum values of these determine the range of possibility for each of the inputs. Since the patchy oil slick model contains the most realism, it is used to run all possible combinations of the input parameters. Significant model outputs are defined and the minimum and maximum of these are collected from the multiple runs of the patchy slick model.

In effect this approach presumes that the statistical distribution of each parameter is uniform. This distribution is said to be useful “..when an expert is only willing/able to estimate an upper and lower bound for a quantity...” and “...is used frequently in exposure assessment.” (Cullen and Frey, 1999, page 71).

As the initial approach to uncertainty analysis of the ERO³S model, six parameters were assumed to be variable: source location, spill rate, spill duration, current speed, wind speed and temperature. With this selection of inputs there are two values each for six parameters: the minimum value and the maximum value. This leads to a total of 2⁶ or 64 unique combinations of parameters. This calculation highlights an assumption of this method: That each parameter value is equally likely and can occur in combination with each other parameter value. In other words that each parameter is uniformly distributed and uncorrelated. The outcomes of interest were picked for this initial approach were the volume of floating oil, areal extent of the oil slick, volume of potentially beached oil and volume of dispersed oil. Because differing parameter sets produce the best and worst case results for each of these outputs, there generally is no generic worst case parameter set: the worst case parameter set depends, rather, on the output of interest.

Example

An example uncertainty analysis is presented in the on-line users guide (see Section 3 User's Guide). In this example dispersant is applied at three times (4, 10 and 13 hours) after the an oil spill begins. For each application, 1000 gallons of dispersant is available and is applied to all floating oil. Table 3 shows the values of five variable parameters used in the analysis. The spill location also varied by 2 minutes and 30 seconds of longitude.

Parameter	Minimum Value	Maximum Value
Leak Rate (gal/day)	1000	2000
Duration (days)	1.0	1.5
Wind (knot)	1	5
Current Speed (m/s)	0.001	0.005
Temperature (°C)	1	5

Table 3 Variable parameters for uncertainty analysis example.

In this case the patchy oil slick model required roughly 90 seconds to execute for each simulation and a total of 64 simulations were performed. Thus the total execution time is approximately 1.5 hours for this example. From these three outputs were selected: volume of floating oil, oil extent and volume of dispersed oil. For each of these the minimum and maximum values were recorded by the model. Table 4 shows that the resulting range of these outputs, for this case, can range by as much as an order of magnitude.

Outcome	Minimum	Maximum
Floating Oil	658 gal	2368 gal
Extent	$3.78 \times 10^9 \text{ ft}^2$	$4.08 \times 10^9 \text{ ft}^2$
Dispersed Oil	317 gal	687 gal

Table 4 Example uncertainty analysis results.

3. User's Guide

The user's guide for the ERO³S model is available on-line by following the links at the EPA web site: <http://www.epa.gov/athens/research/projects/eros.3> A short introduction is given here.

Applet versus Application

The model is supplied in two forms: 1) a simplified version that runs as an "applet" from the EPA web site, 2) the full version that runs as an "application" on the user's computer. The applet version is limited in that it does not access databases, nor allow for saving of inputs or outputs. Conversely, the application version will provide these functions and will be downloaded from the EPA web site at <http://www.epa.gov/CEAM>.

Software Requirements

The applet version of ERO³S runs within browser windows. Either Microsoft's Internet Explorer or Netscape Navigator are suitable. An additional requirement, however, is that the Java Run-Time Environment is equal to that used to create ERO³S. The required version is Sun Java 2 v1.4.2_05 or higher, which is available from <http://java.com/en/index.jsp>.

If Microsoft Internet Explorer is used, then the SUN Java plug-in must be selected as shown in Figure 6.

Basic Interface Options

The interface contains three introductory screens that are shown in Figures 7, 8, and 9. The identification screen (Figure 8) can be used to record general information concerning the spill and simulation.

The first step toward running the model is to select the code (Figure 9). As noted above, there are four choices in the ERO³S framework:

1. Empirical Dispersant Data -- Explore the character of the empirical dispersant data.

³ Temporarily and for the purposes of peer review of this document, access is granted only to selected reviewers at <http://intranet.epa.gov/nerlintr/athens/research/projects/oilspills/index.html>. Permanent access will be provided at the address given above in the text.

2. Laboratory Flask Simulation -- Perform a simulation of the baffled flask experiment with dispersant application at varying times.
3. Patchy Oil Slick Model -- Simulate the movement of an oil slick composed of individual patches and disperse at specified times
4. Uncertain Patchy Oil Slick Model -- Evaluate the uncertainty associated with some of the input parameters of the patchy oil slick model.

The applications build in complexity and use components from lower-numbered models. A realistic oil slick should be simulated with the fourth or fifth options: (the patchy oil slick models) as the prior models are too limited for most situations.

When the selection of one of the four has been made, more screens are added to the interface. (See Figure 10, for an example.) These will include all necessary input and output screens for the selected model. Changing the model selection causes the interface to reconfigure itself for the newly-selected option. All previous information is lost when a new selection is made. This effect, in fact, can be useful to assure that all old results have been cleared from the model.

Since each model contains an example problem, the "Run" button can be pushed anytime after the model selection has been made. (The button can also be pushed before a selection is made, but there won't be any calculations made.) Changes to the model inputs are made on each input screen, prior to running the model. There are three things to know about the current version of the model:

1. This "applet" version of the model does not allow storage of data. This is a requirement of running from the Intranet (or Internet). Later a PC version of the model will be supplied that will allow storage and retrieval of data.
2. Most inputs in this version are selected by choosing from "drop-down" lists. The PC version of the model will allow direct input of numerical values.
3. The source code for the model is about 500 pages long when printed and requires a download of approximately 364 kbytes.

Specific instructions for each of the four ERO³S options are given in the on-line user's guide.

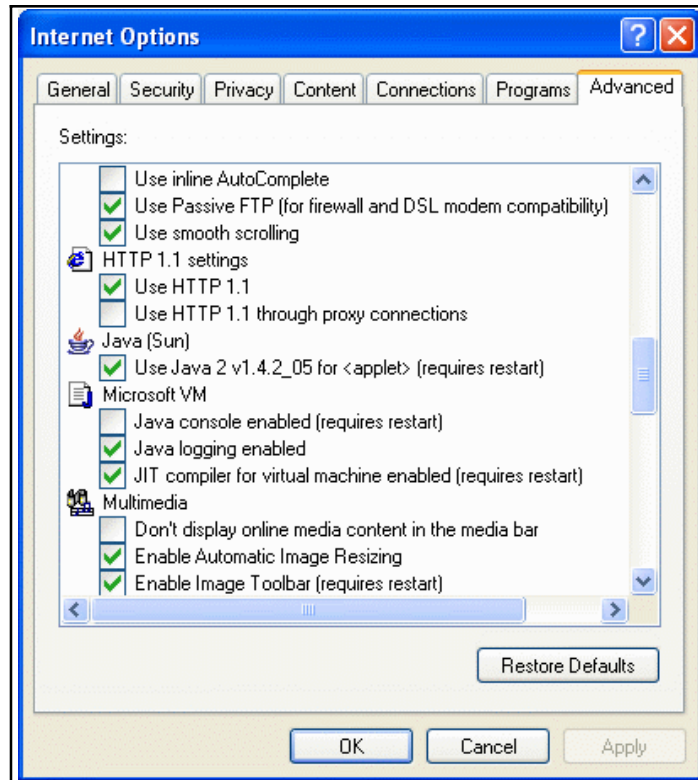


Figure 6 Required options for use of ERO³S in Microsoft Internet Explorer.

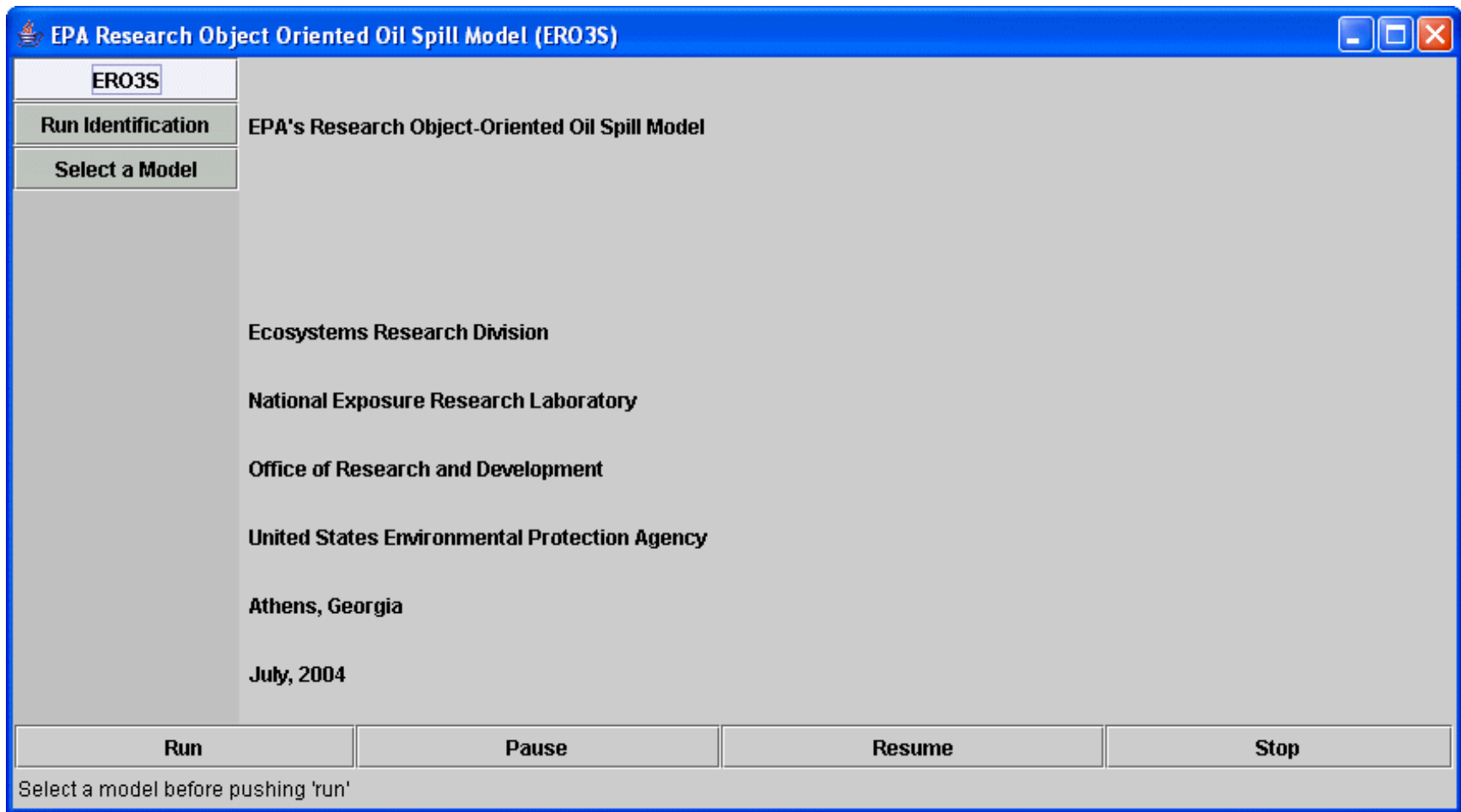


Figure 7 Introductory ERO³S screen.

EPA Research Object Oriented Oil Spill Model (ERO3S)

ERO3S

Run Identification

Select a Model

Spill Name

Spill Location

Spill Date

User Name

Simulation Date

Comment

Run **Pause** **Resume** **Stop**

Select a model before pushing 'run'

Figure 8 ERO³S identification screen.

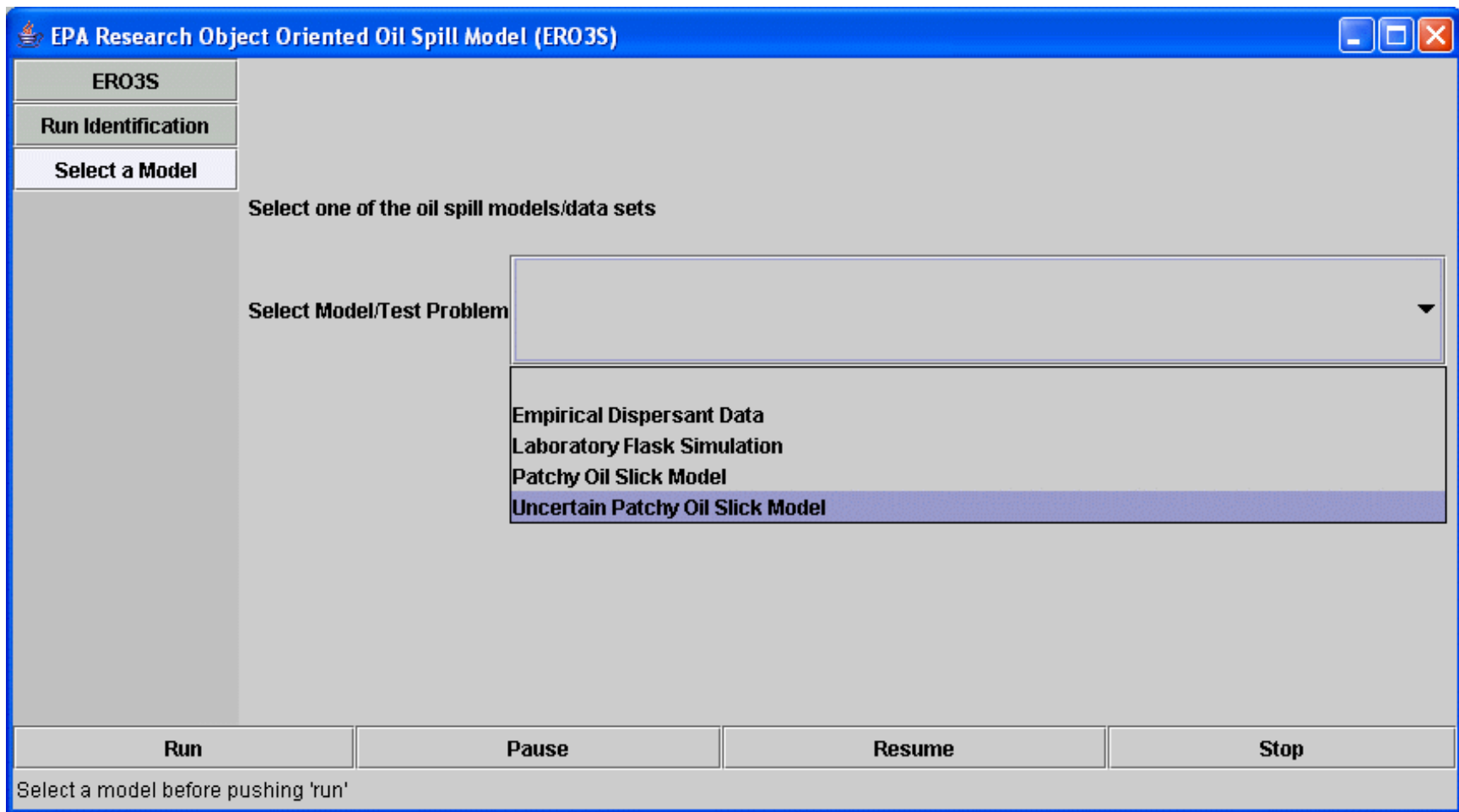


Figure 9 ERO³S model selection screen.

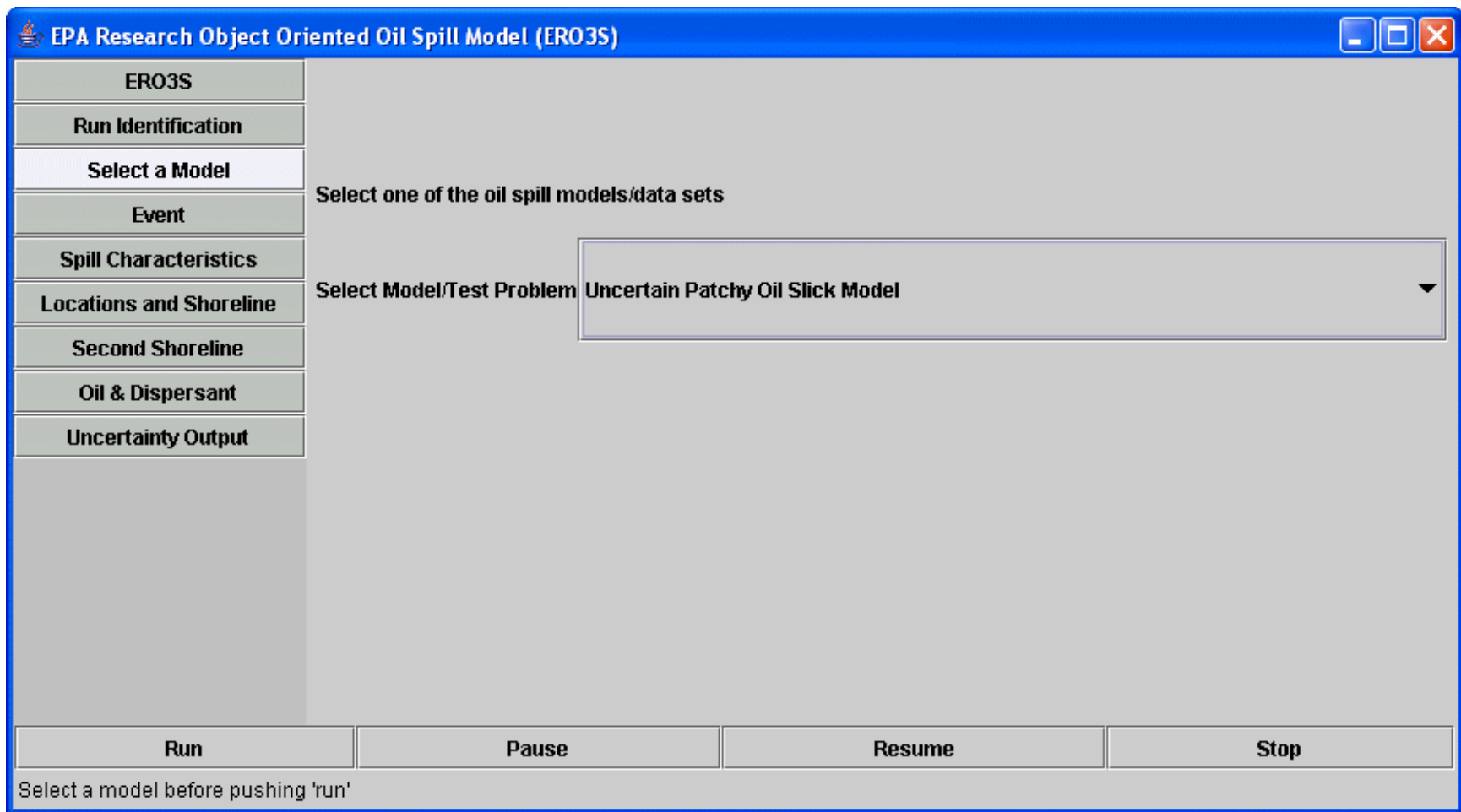


Figure 10 ERO³S model screen example.

4. Conclusions

EPA's Object-Oriented Oil Spill (ERO³S) model was developed to create a public-domain model for the purpose of oil spill response planning. The model contains a suite of four applications that range from an exploration of laboratory scale dispersant effectiveness data through a patchy oil slick model to an uncertainty calculation that addresses fundamental and irreducible limitations to oil spill model applications.

The primary focus of the work presented herein was to establish a framework for developing and evaluating various formulations of oil spill models. Work is continuing in several areas:

1. Inclusion of alternate weathering models and databases (including Stiver and MacKay, 1984 and Stiver et al. 1988),
2. Expansion of physio-chemical phenomena included in the model,
3. Inclusion of alternate spreading formulations (including those of Lehr et al., 1989 and Buckmaster (1972): equation 13), and
4. Enhancement of the graphical user interface

Because of the established structure of the model, this work represents incremental enhancement. Each feature that is to be included can be encapsulated as a separate object and used to modify one or more of the existing four applications contained in ERO³S or used to create new applications that add to the four.

Future work will address linking of the model to existing water quality and hydrodynamic models, testing against spill data and inclusion of new approaches to estimating the impacts of dispersants on oil slicks.

References

- Buckmaster, J., 1973, Viscous-gravity spreading of an oil slick, *J. Fluid Mech*, 59(3), 481-491.
- Canevari, G.P., 1969, The role of chemical dispersands in oil cleanup, in *Oil on the Sea*, David. P. Hoult, ed., Plenum Press, New York, 29-51.
- Cullen, A. C., and H.C. Frey, 1999, *Probabilistic Techniques in Exposure Assessment*, Plenum Press, New York, 335pp.
- Environment Canada, 1999, *A Catalogue of Crude Oil and Oil Product Properties*, Environmental Technology Center, Emergencies Science Division, Environment Canada, www.etcentre.org.
- Fay, J.A., 1969, The spread of oil slicks on a calm sea, in *Oil on the Sea*, David. P. Hoult, ed., Plenum Press, New York, 53-63.
- Felthberg, E., 1969, Low-Order Classical Runge-Kutta Formulas with Stepsize Control and Their Application to Some Heat Transfer Problems, NASA, Technical Report R-315.
- Fingas, M., 2001, *The Basics of Oil Spill Cleanup*, Lewis Publishers, Boca Raton, 233 pp.
- Hairer, E., S.P. Norsett, and G. Wanner, 1993, *Solving Ordinary Differential Equations I, Nonstiff Problems*, Second Revised Edition, Springer Verlag, New York, 528 pp.
- Hoult, 1972, Oil Spreading on the Sea, *Annual Reviews of Fluid Mechanics*, 4, 341-368.
- Li, W.H. and S. H. Lam, 1976, *Principles of Fluid Mechanics*, Addison-Wesley, Reading, Massachusetts, 374pp.
- Meyer, B., 1997, *Object Oriented Software Construction*, 2ed, Prentice Hall, Upper Saddle River, New Jersey, 1254 pp.
- Oreskes, N, et al., 1994, Verification, Validation, and Confirmation of Numerical Models in the Earth Sciences, *Science*, 263, 641.
- Sorial, G., C., Chandrasekar, and J. W. Weaver, 2004, *Characteristics of Spilled Oils, Fuels, and Petroleum Products: 2a. Dispersant Effectiveness Data for a Suite of Environmental Conditions – The Effects of Temperature, Volatilization, and Energy*, United States Environmental Protection Agency, National Exposure Research Laboratory, EPA/600/R-04/xxx.

- Stiver, W., and D. Mackay, 1984, Evaporation rate of spills of hydrocarbons and petroleum mixtures, *Environmental Science and Technology*, 18(11), 834-840.
- Stiver, W., W.Y. Shiu, and D. Mackay, 1989, Evaporation times and rates of specific hydrocarbons in oil spills, *Environmental Science and Technology*, 23(1), 101-105.
- U.S. Coast Guard, 1994, Adios Automated Data Inquiry for Oil Spills, Version 1.1, National Oceanic and Atmospheric Administration, Hazardous Materials Response and Assessment Division, Seattle, Washington, 98115
- U.S. Environmental Protection Agency, 1993, Understanding Oil Spills and Oil Spill Response, EPA 540-K-93-003.
- U.S. Environmental Protection Agency, 2003, Draft Guidance on the Development, Evaluation and Application of Regulatory Environmental Models, Council on Regulatory Environmental Modeling, Office of Science Policy, USEPA,
- Wang, Z., B.P. Hollebone, M. Fingas, B. Fieldhouse, L. Sigouin, M. Landriault, P. Smith, J. Noonan, and G. Thouin, 2003, Characteristics of Spilled Oils, Fuels, and Petroleum Products: 1. Composition and Properties of Selected Oils, United States Environmental Protection Agency, National Exposure Research Laboratory, EPA/600/R-03/072.

Appendices

Acronyms

2FO	No. 2 Fuel Oil
BFT	Baffled Flask Test
ERO ³ S	EPA's Research Object-Oriented Oil Spill Model
EPA	Environmental Protection Agency
GUI	graphical user interface
GPS	global positioning system
MDP	Model Development Platform
ODE	ordinary differential equation
PBC	Prudhoe Bay Crude
RKF	Runge-Kutta-Felhberg
SLC	South Louisiana Crude

Appendix: Latitude-Longitude Coordinates in ERO³S

Geographic locations are indicated in ERO³S with latitude-longitude⁴ coordinates. Latitudes are measured from the equator and are assumed to increase positively to the North. Longitudes are measured from the prime meridian and assumed to increase positively to the West. So that the longitudes used in ERO³S are longitudes “west”. Figure 11 shows the data-entry screen for the locations of the stern of the ship (or other oil container) and 10 shoreline points. These locations are presumed to be available from a global positioning system (GPS) receiver and/or a nautical chart. The resulting shoreline is shown in Figure 12. These data show the Great South Bay of Long Island New York between Oakdale and Moriches.

	Degrees	Minutes	Seconds	Degrees	Minutes	Seconds
Stern of Ship	40.0	42.0	0.0	73.0	6.0	30.0
Shore Line Point - 0	40.0	42.0	0.0	73.0	9.0	0.0
Shore Line Point - 1	40.0	43.0	15.0	73.0	8.0	0.0
Shore Line Point - 2	40.0	43.0	10.0	73.0	6.0	0.0
Shore Line Point - 3	40.0	43.0	50.0	73.0	2.0	0.0
Shore Line Point - 4	40.0	45.0	0.0	73.0	1.0	0.0
Shore Line Point - 5	40.0	44.0	45.0	72.0	58.0	50.0
Shore Line Point - 6	40.0	44.0	40.0	72.0	56.0	50.0
Shore Line Point - 7	40.0	45.0	30.0	72.0	55.0	10.0
Shore Line Point - 8	40.0	45.0	20.0	72.0	54.0	0.0
Shore Line Point - 9	40.0	45.0	20.0	72.0	54.0	0.0

Figure 11 Illustration of latitude-longitude input for ship location and locations of shore line points.

⁴Abbreviated as lat-long.

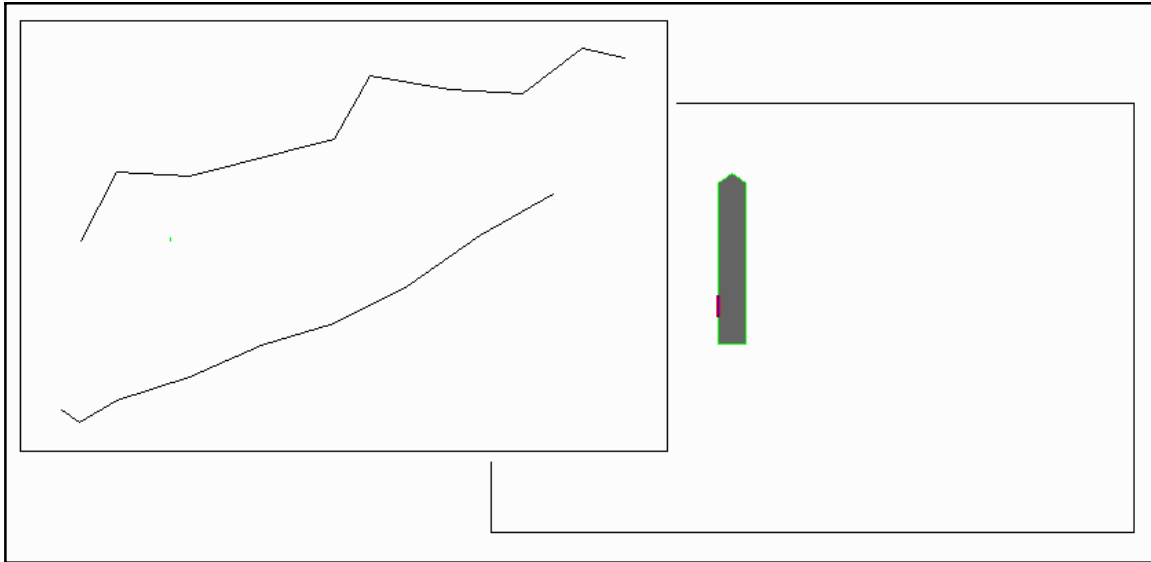


Figure 12 Shorelines entered from lat-long data. The top shoreline's coordinates are shown in Figure 11. The ship itself is barely visible between the two shorelines, but can be seen in the close up at right.

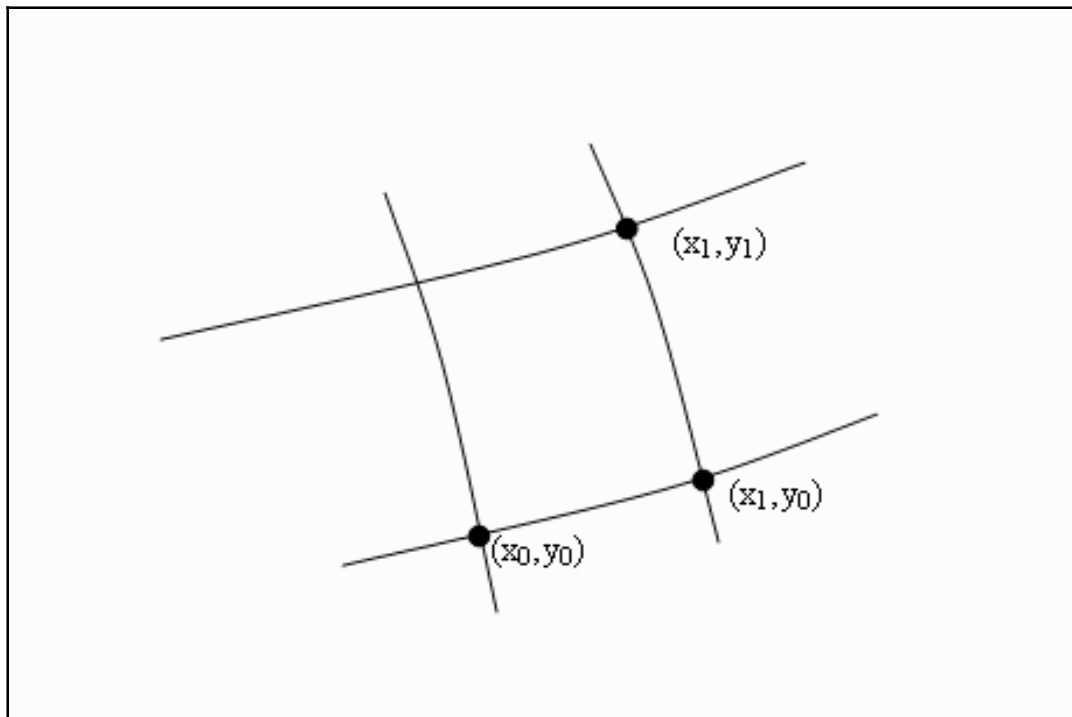


Figure 13 Latitude-Longitude calculation in ERO³S.

Figure 13 illustrates the points involved in calculating the distance between two lat-long points. Because the distance between any two lines of longitude depends upon the latitude, the

difference in longitude is calculated by assuming that points are at the latitude of a) the first point (x_0) and b) the second point (x_1). These two results are averaged to obtain the difference in East-West direction. The North-South distance is calculated simply from the difference in longitude.

Appendix: Model Development Within the MDP Model Development Platform

The ERO³S model was developed within the MPD model development platform. This platform facilitates the creation of object-oriented models in the Java programming language. MDP includes components for

- automated generation of Graphical User Interfaces (GUIs)
- selection from among a number of related models under a single interface
- access to a series of numerical solvers including,
 - a family of Runge-Kutta-Fehlberg (RKF) Ordinary Differential Equation (ODE) solvers
 - a linear equation solver
 - an uncertainty range solver
- graphical display routines for both animated drawings and charted output

The correct usage of the MDP platform gives a flexible approach to creating and solving model equations.

Procedural Outline for Creating MDP Applications

Each MDP application contains several required files/classes:

- Main routine,
- Applet frame,
- Application frame,
- One or more interfaces,
- One or more models,
- Title Screens, and
- Background Screens.

Directory and Package Structure

Java requires that file names and directory structures match the internal package structure of an application. The structure that has been created for MDP applications and applets⁵ is

⁵In Java applications are codes that run on PCs in much the same fashion as any other windows software. Applets run as embedded objects in web pages. Applets are subject to a series of constraints, both security-related and practical, that limit their comprehensiveness. For brevity both applications and applets will be indicated by use of the term application. Where necessary to distinguish between the two, the context will clearly indicate which is indicated.

shown in Figure14. The general components of MDP are located in the directory/package modelsjavabase and are separate from any application. MDP contains basic utilities for creating and running applications in Java. MDP contains:

- Graphical User Interface (GUI) components in the fw2 subdirectory,
- charting software in the MSBChart and GraphControl subdirectories,
- general purpose drawing software in the graphics subdirectory,
- numerical methods in the models and Numerics subdirectories, and
- various utilities in the utils subdirectory.

ERO³S components are contained in the directory/package ERO3S, likewise separate from MDP and any other application. ERO³S consists of three parts:

- EmpiricalDispersantData,
- EROS, and
- OilSlick.

EmpiricalDispersantData contains results from the dispersant studies of Sorial et al. (2004). These are used as the basis for dispersing oil slicks in ERO³S. EROS contains the main routines that run the model. OilSlick contains the single and multiple oil slick implementations of the model.

The structure shown in Figure 14 organizes the source code (subdirectory src), Java class files (classes), documentation (doc), backup (bak) into standardized locations for any MDP application. The subdirectories gov and epa under src and classes follow Java naming convention and trace the codes back to development within the [Federal] EPA. Figure15 shows the structure within “classes” and how it is mimics the structure of src. Unlike “src”, “classes” is automatically generated upon compilation when using Borland’s JBuilder for creating applications. Thus the major chore in setting up an application is creating the bak, doc, classes and src directories, then placing source codes in subdirectorys:

src/gov/epa/*first level name/second level name*

where the *first level name* is chosen by convention to match the application name (i.e., ERO3S) and as many *second level names* as needed are added to match sub parts of the application (i.e., EmpiricalDispersantData, OilSlick, etc.)

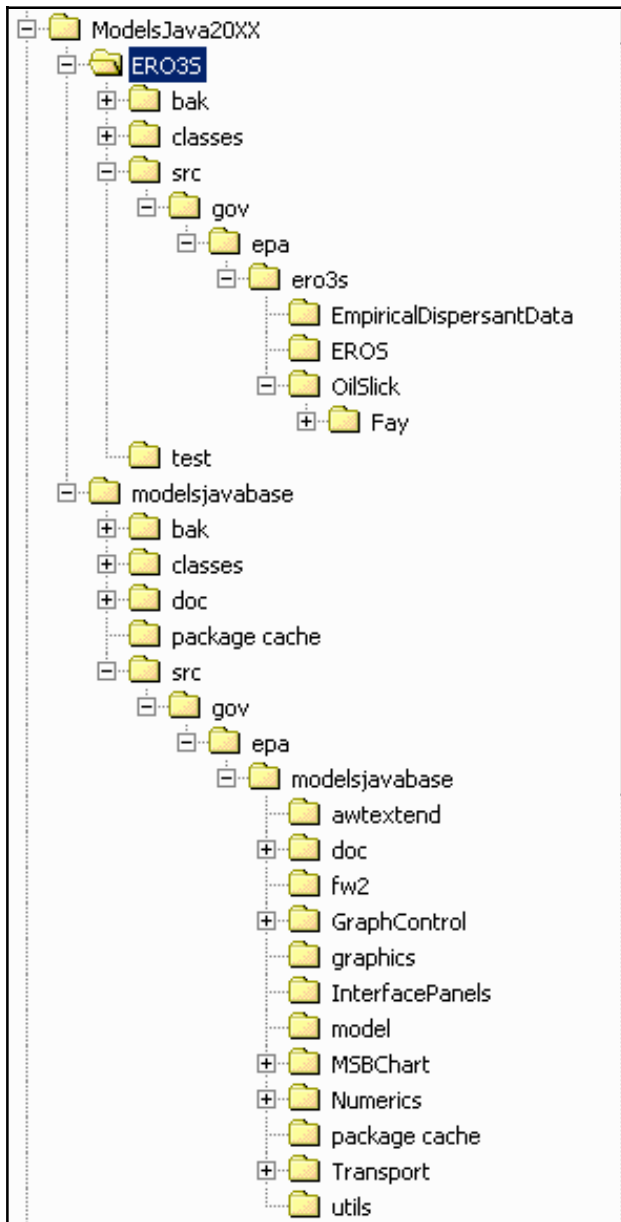


Figure 14 Directory structure of the ERO³S MDP application. The two first level directories, ERO3S and modelsjavabase, are the locations that contain the code that is unique to ERO³S (ERO3S) and the MDP framework (modelsjavabase).

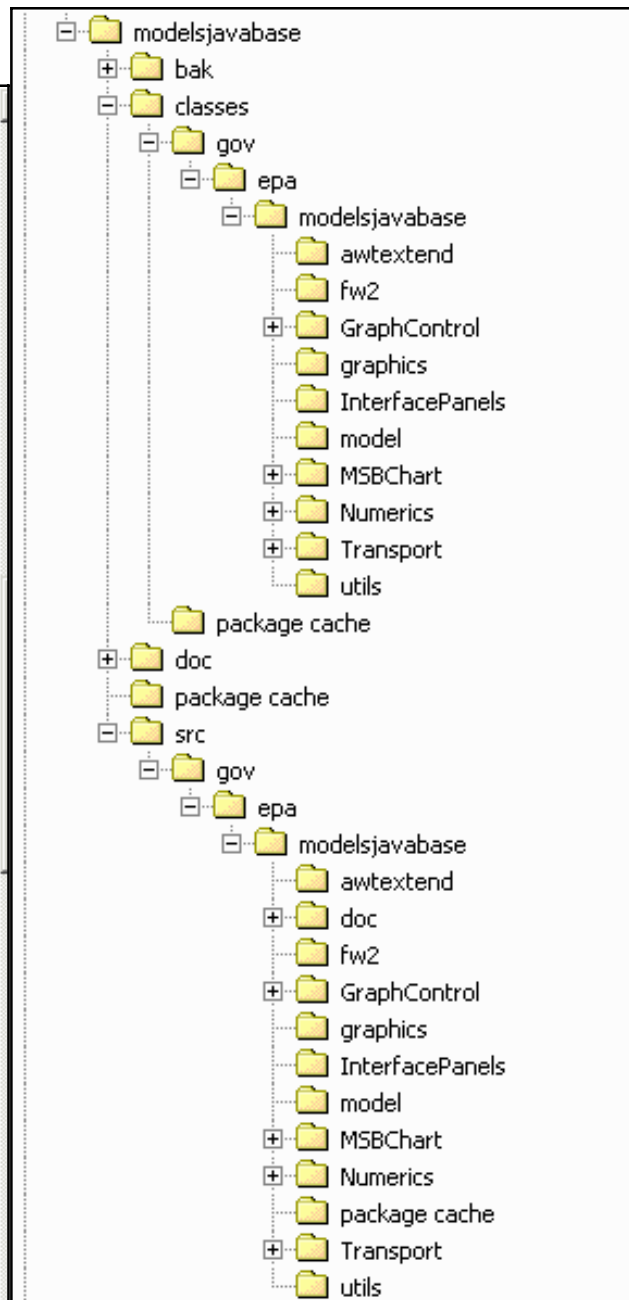


Figure 15 Directory structure of the Java MDP showing the required subdirectories: bak, classes, doc, package cache, and src. An src subdirectory is created by the MDP user for each new model and must contain additional subdirectories: gov, epa, first level name (here: modelsjavabase), and second level names (here: awtextend, doc, fw2, etc).

Appendix: Sorial et al. (2004) Dispersant Data

A linear regression empirical model was fit to the experimental data of Sorial et al., (2004) for each of the oil/dispersant combinations. The model takes the following form and is used directly in each ERO³S application:

$$\begin{aligned}
 \% \text{ Efficiency}_{oil:dispersant} = & \beta_0 + \beta_w w + \beta_t t + \beta_s s \\
 & + \beta_{wt} w t + \beta_{ws} w s + \beta_{ts} t s + \beta_{wts} w t s \\
 & + \beta_{w^2} w^2 + \beta_{t^2} t^2 + \beta_{s^2} s^2 \\
 & + \beta_{w^2 t^2} w^2 t^2 + \beta_{w^2 s^2} w^2 s^2 + \beta_{t^2 s^2} t^2 s^2 + \beta_{w^2 t^2 s^2} w^2 t^2 s^2
 \end{aligned} \tag{38}$$

where w represents weathering in %, t is the temperature (water) in °C, and s is the speed in RPM. The terms were chosen to include linear and parabolic effects of each variable and possible two- and three-factor interactions. If all were statistically significant, the model would include 15 terms. Because for each oil/dispersant combination there are no more than 27 data points, no additional interaction or non-linear terms were included in the model. Data from the replicate study were used to enhance the regressions: each non-replicated point for the speed of 200 rpm and dispersants “A” and “B” was replaced by the average result from the replicate study. As seen in the results, only a few terms were significant for a given oil/dispersant combination as determined by step-wise multiple regression with an acceptance/rejectance level of 0.05. Between 4 and 9 terms represented the data for these experiments. Notably the step-wise regression showed that adding more of the 15 possible terms did not improve the fits.

The various parameters of Equation 38 for the various oil - dispersant combinations are given in Table 5 together with R^2 values, which indicates the linearity of the model. Generally, values above 90% indicate good linear fits. With the exception of 2FO with no dispersant (86.9%), all the R^2 values were above 90%. Regression equation terms that include weathering as a variable are highlighted in Table 5 with gray shading. Note from the table that none of the regressions include weathering alone as a term. This indicates the secondary nature of weathering as a variable as described previously for each oil. Figures 16 to 24 show comparisons of estimated and measured values of dispersal efficiency. Each of the plots show that the data cluster along the 1:1 line, indicating, obviously, a close match. Prudhoe Bay Crude with either dispersant (Figures 19 and 22) and the South Louisiana Crude with dispersant B (Figure 24) show particularly tight clustering along this line.

Table 5 Coefficients of Regression Equations with Terms Determined by Step-Wise Linear Regression

Factor ⁽¹⁾	Prudhoe Bay Crude			No. 2 Fuel Oil			South Louisiana Crude		
	No Dispersant	Dispersant A	Dispersant B	No Dispersant	Dispersant A	Dispersant B	No Dispersant	Dispersant A	Dispersant B
constant	-5.9325	-264.6	-15.16	1.490	-112.0	-17.65	-17.25	41.39	-69.24
w									
t	1.2090	4.222	3.506		10.67	3.032	-0.1381	-8.873	-9.149
s		2.609			0.6617		0.1680	0.1762	1.322
w t			-8.386e-3				-6.391e-3		
w s				-2.452e-3				-1.631e-3	
t s	-4.120e-3		-8.386e-3	-1.4089e-3	-2.435e-2		7.656e-4	4.092e-2	4.132e-2
w t s			-4.845e-5						
w ²		-1.038e-2							
t ²	-1.979e-2	-9.697e-2	-2.817e-2	6.996e-3	-0.2000	-6.313e-2	4.382e-3	0.1516	0.1178
s ²	1.468e-4	-5.409e-3	1.433e-3	9.871e-5		1.256e-3	-3.3750e-4		-2.970e-3
w ² t ²							9.99e-6		
w ² s ²				1.39e-6			5e-8		
t ² s ²	2.6e-7			9e-8	1.30e-6			-2.87e-6	-2.26e-6
w ² t ² s ²									
R ²	91.1%	97.5%	98.2%	86.9%	96.7%	94.8%	98.2%	90.8%	98.6%

⁽¹⁾ w = weathering, t = temperature, s = speed

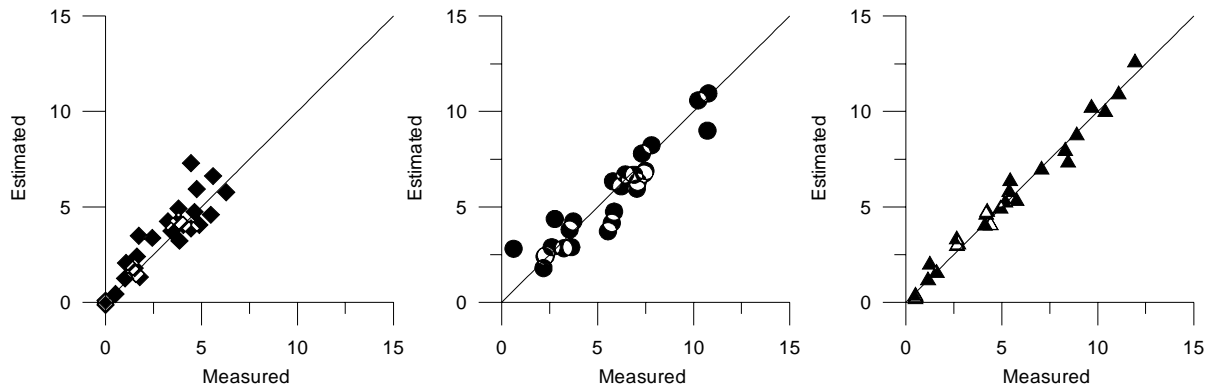


Figure 16 Estimated vs Measured % Dispersal of PBC with No Dispersant.

Figure 17 Estimated vs Measured % Dispersal of 2FO with No Dispersant.

Figure 18 Estimated vs Measured % Dispersal of SLC with No Dispersant.

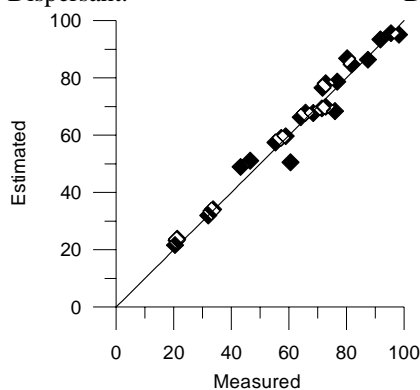


Figure 19 Estimated vs Measured % Dispersal of PBC with Dispersant "A".

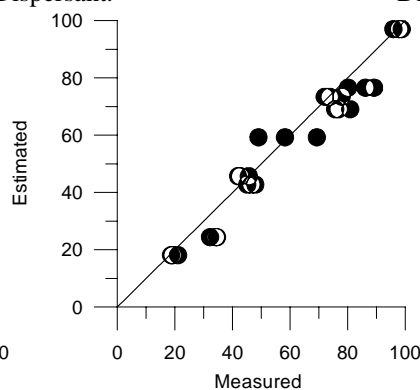


Figure 20 Estimated vs Measured % Dispersal of 2FO with Dispersant "A".

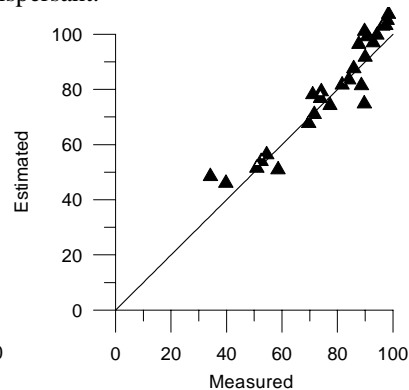


Figure 21 Estimated vs Measured % Dispersal of SLC with Dispersant "A".

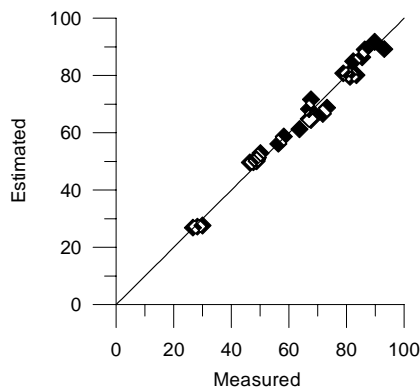


Figure 22 Estimated vs Measured % Dispersal of BPC with Dispersant "B".

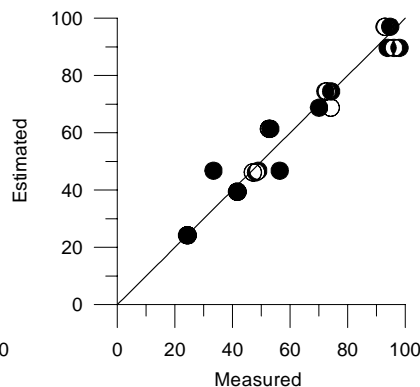


Figure 23 Estimated vs Measured % Dispersal of 2FO with Dispersant "B".

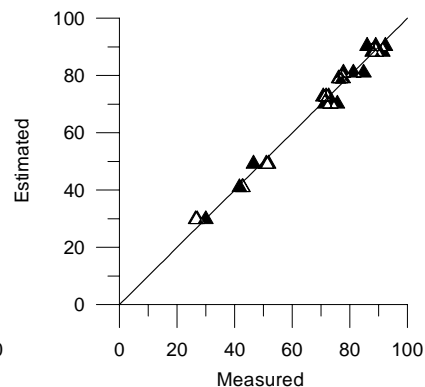


Figure 24 Estimated vs Measured % Dispersal of SLC with Dispersant "B".

Figure 25 shows a comparison of the regression equations and measured values plotted for the Prudhoe Bay Crude with no dispersant. The squares, for example, should cluster about the 200 rpm dashed line. The measured values, however, span almost the entire range of dispersal for speeds of 150 rpm to 250 rpm. This result indicates that the measured variation in dispersal at 200 is as great as the fitting error in the regression equations. The coefficients for these regressions contain no terms that involve weathering. Thus the amount of volatilization weathering that occurs does not affect the dispersal efficiency. So the three curves for the different speeds represent all possibilities for dispersal of the oil.

Figure 26 shows a comparison of the regression equations and measured values plotted for the Prudhoe Bay Crude with dispersant A. The regression equations for this pair contain no terms involving weathering (Table 5), so that the regression equations only need to be plotted for speed and temperature. The graph shows the inverted parabolic shape of the curves (i.e., highest dispersal at the mid-temperature), and the experimental data for each speed and percent weathering. That the latter quantity is unimportant for this oil and dispersant is shown by the data points falling generally near each other regardless of the amount of weathering.

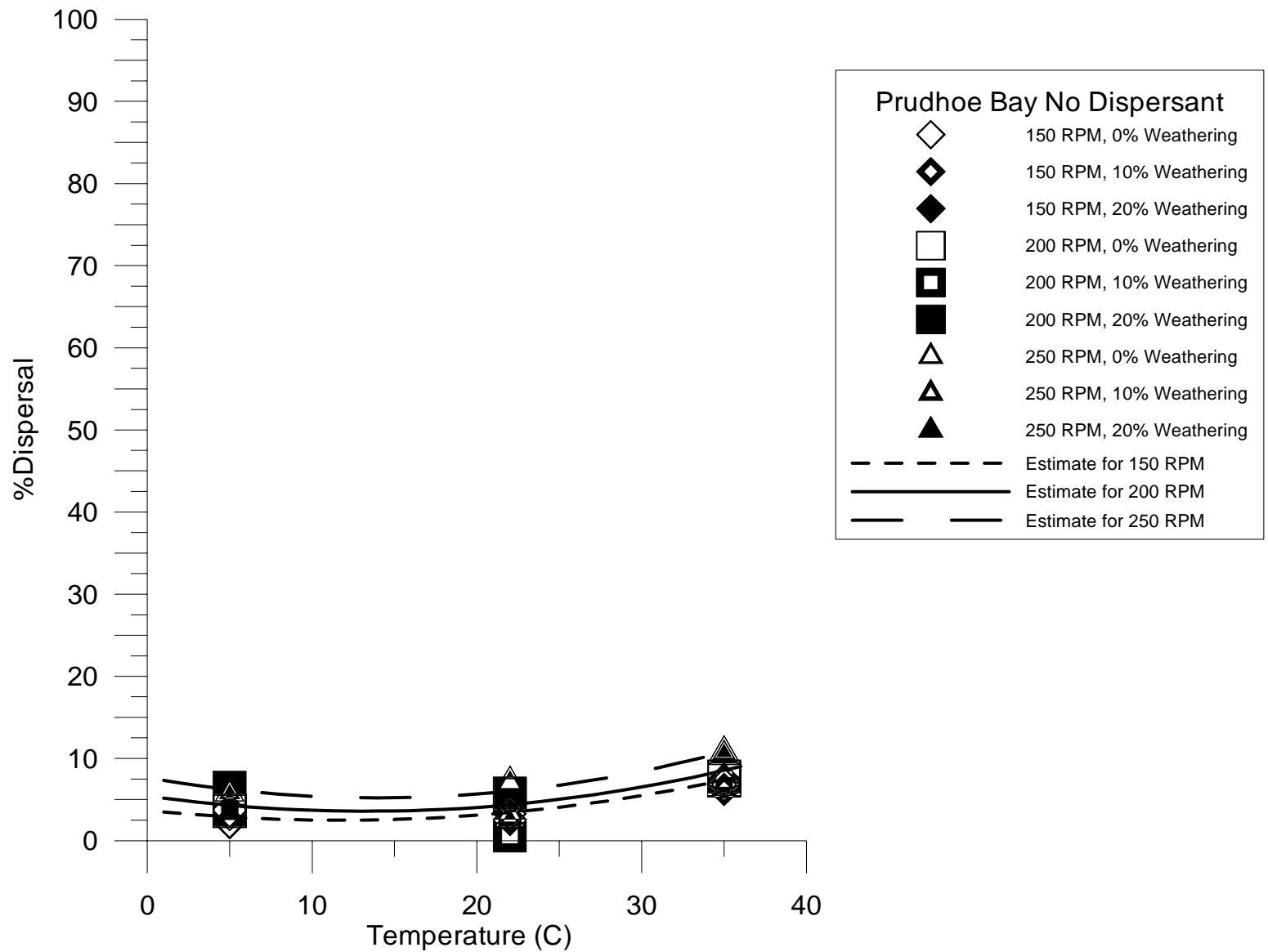


Figure 25 Comparison of regression equations (curves) against measured Prudhoe Bay Crude/no dispersant efficiency.

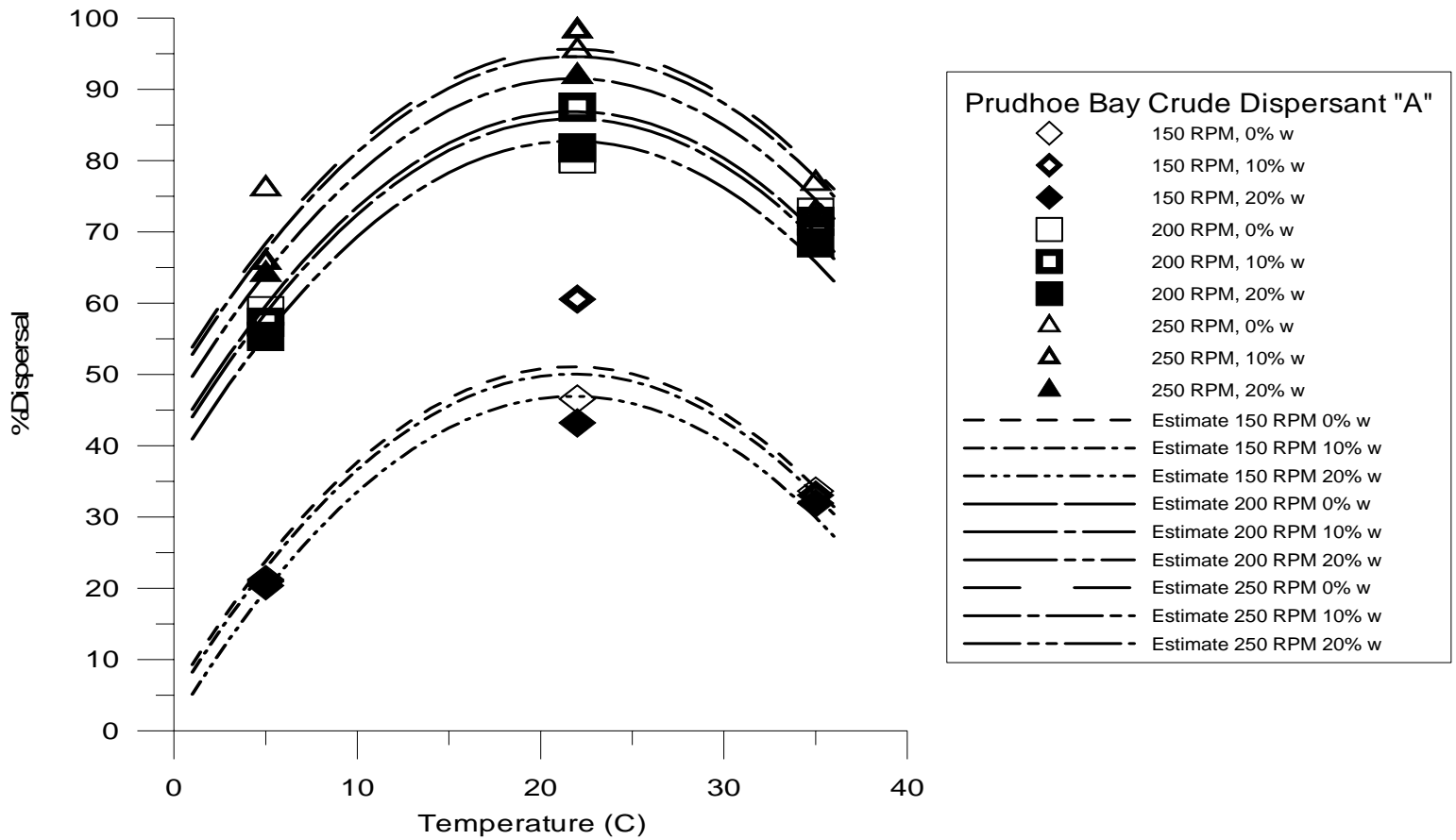


Figure 26 Comparison of regression equations (curves) against measured Prudhoe Bay Crude/dispersant "A" efficiency.

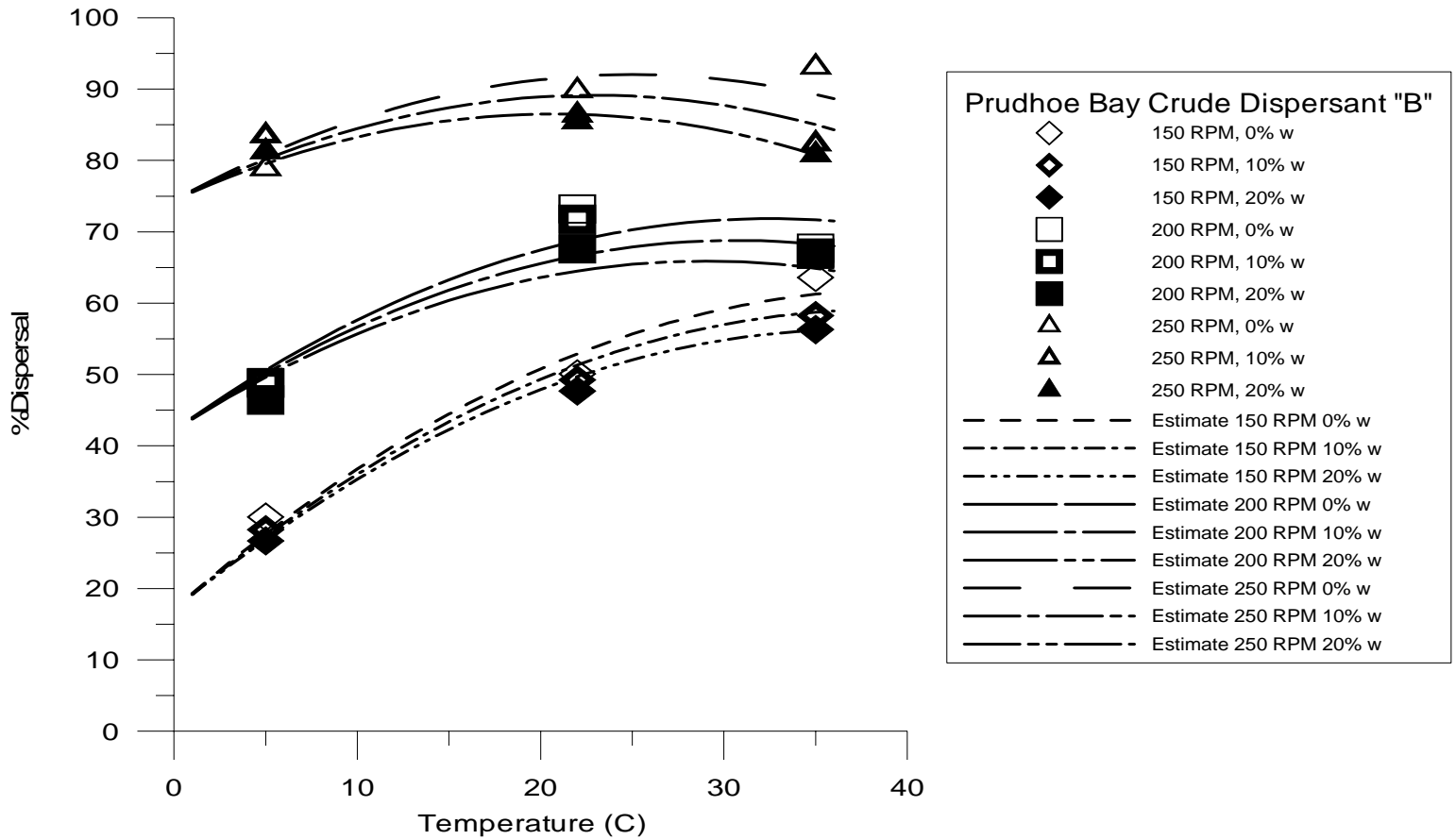


Figure 27 Comparison of regression equations (curves) against measured Prudhoe Bay Crude/dispersant “B” efficiency.

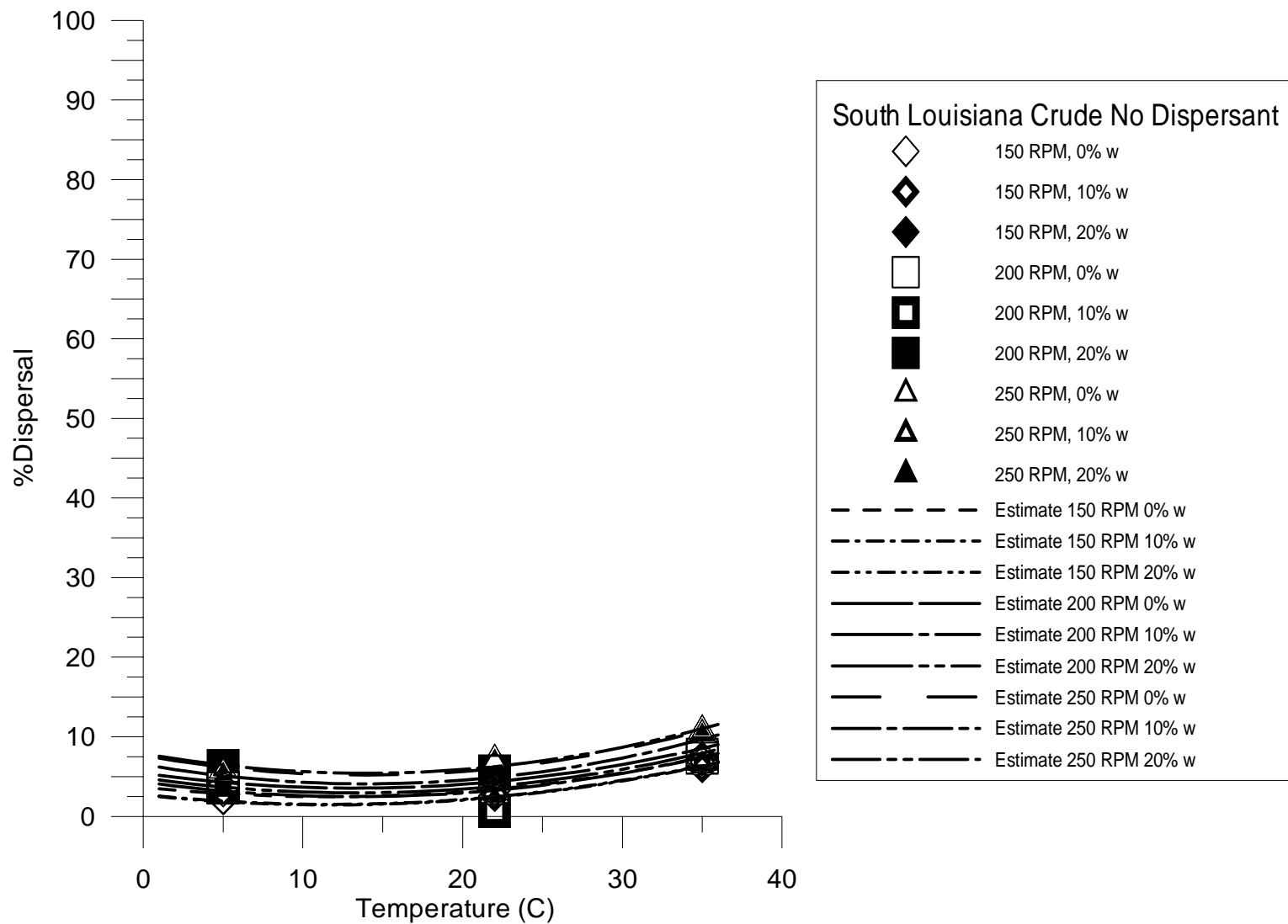


Figure 28 Comparison of regression equations (curves) against measured South Louisiana Crude/No Dispersant efficiency.

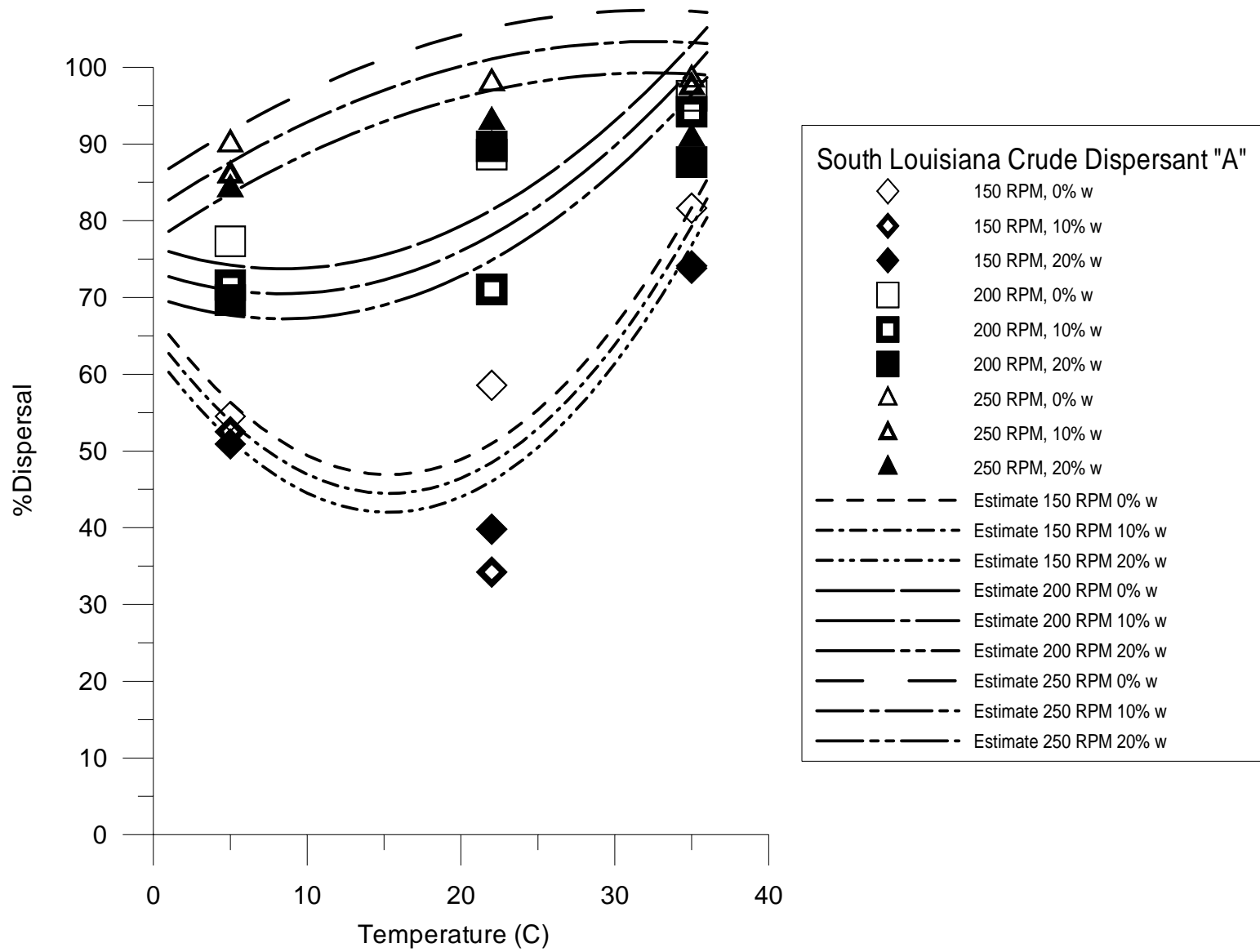


Figure 29 Comparison of regression equations (curves) against measured South Louisiana Crude/Dispersant "A" efficiency.

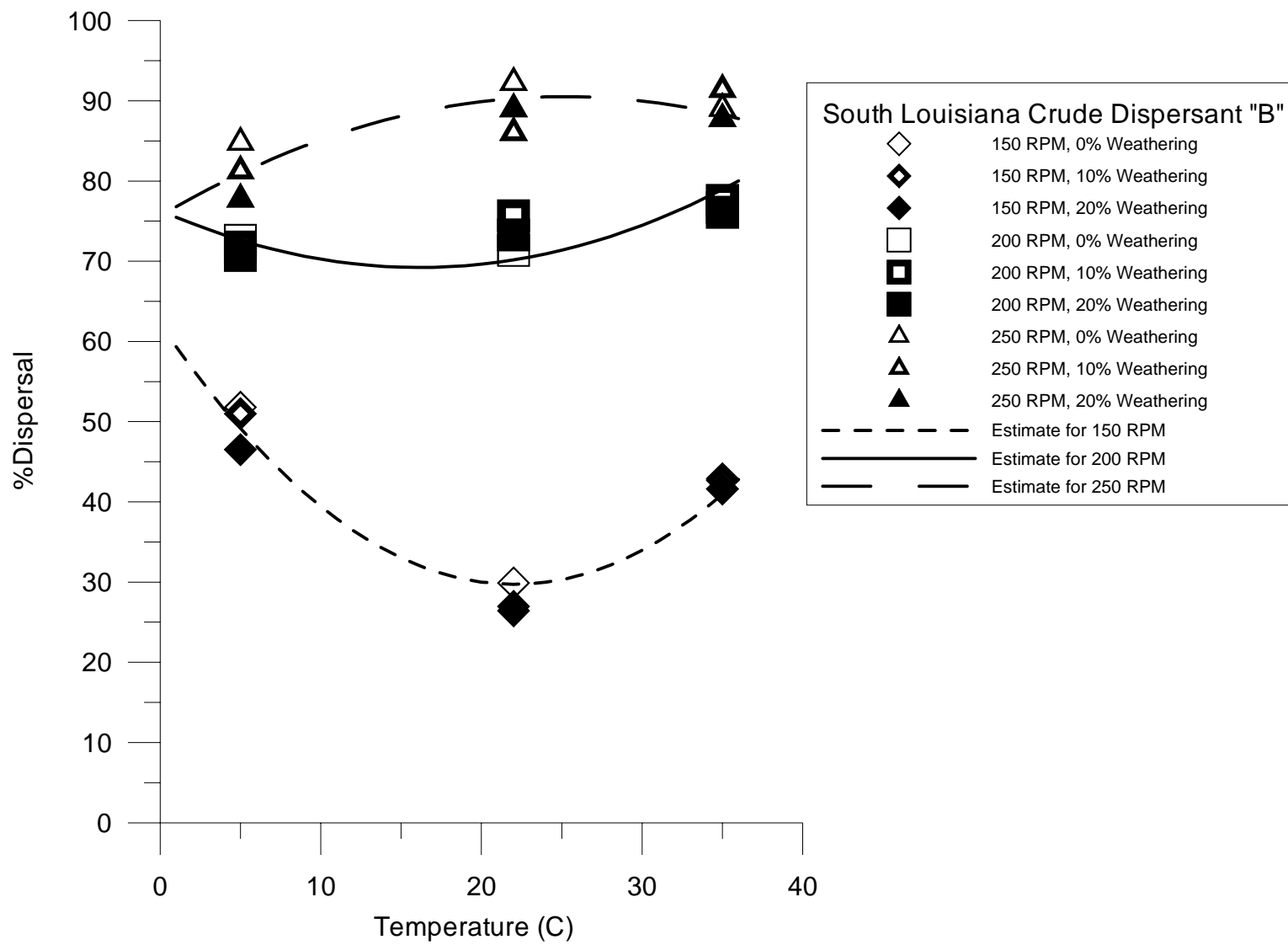


Figure 30 Comparison of regression equations (curves) against measured South Louisiana Crude/Dispersant "B" efficiency.

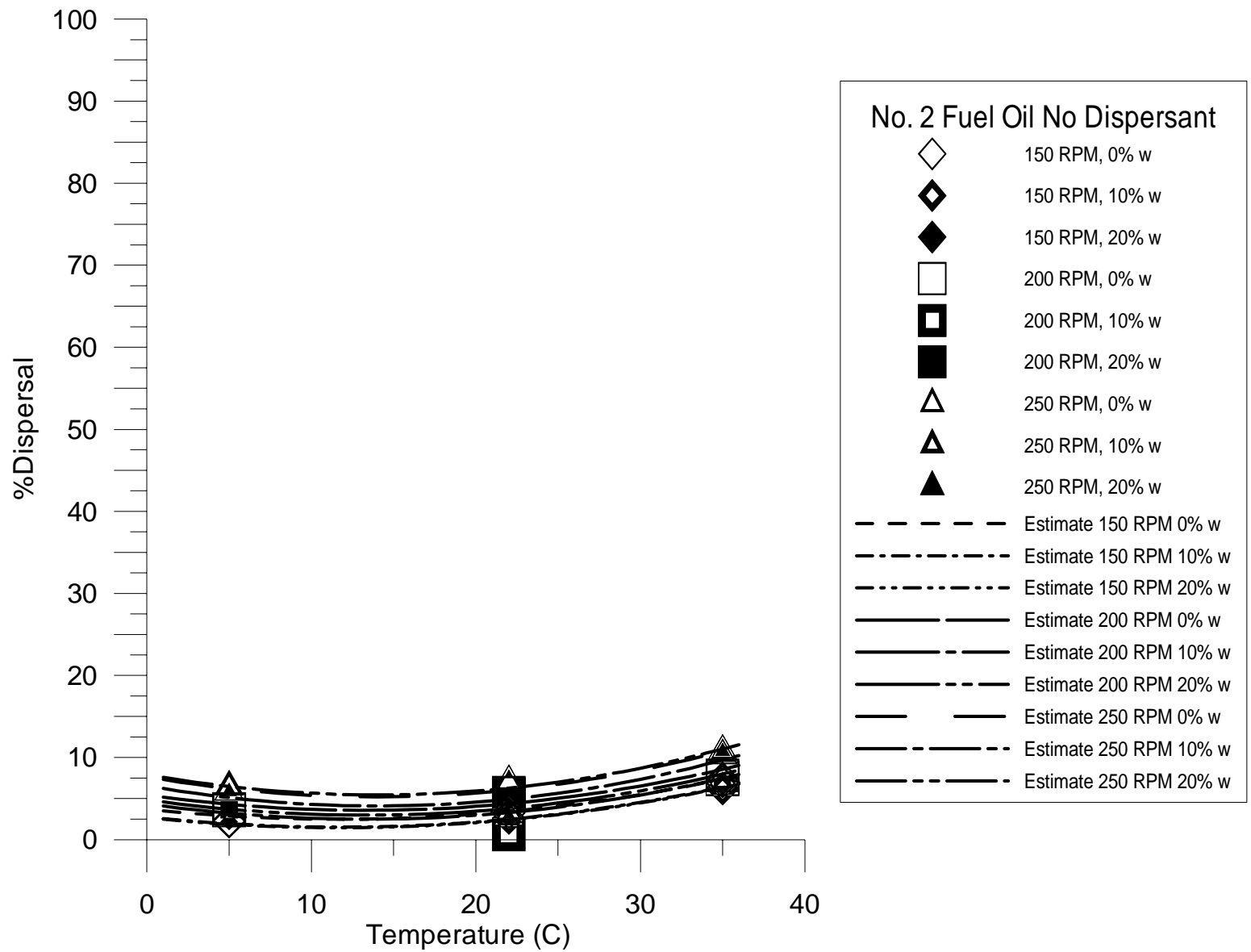


Figure 31 Comparison of regression equations (curves) against measured No. 2 Fuel Oil/No Dispersant efficiency.

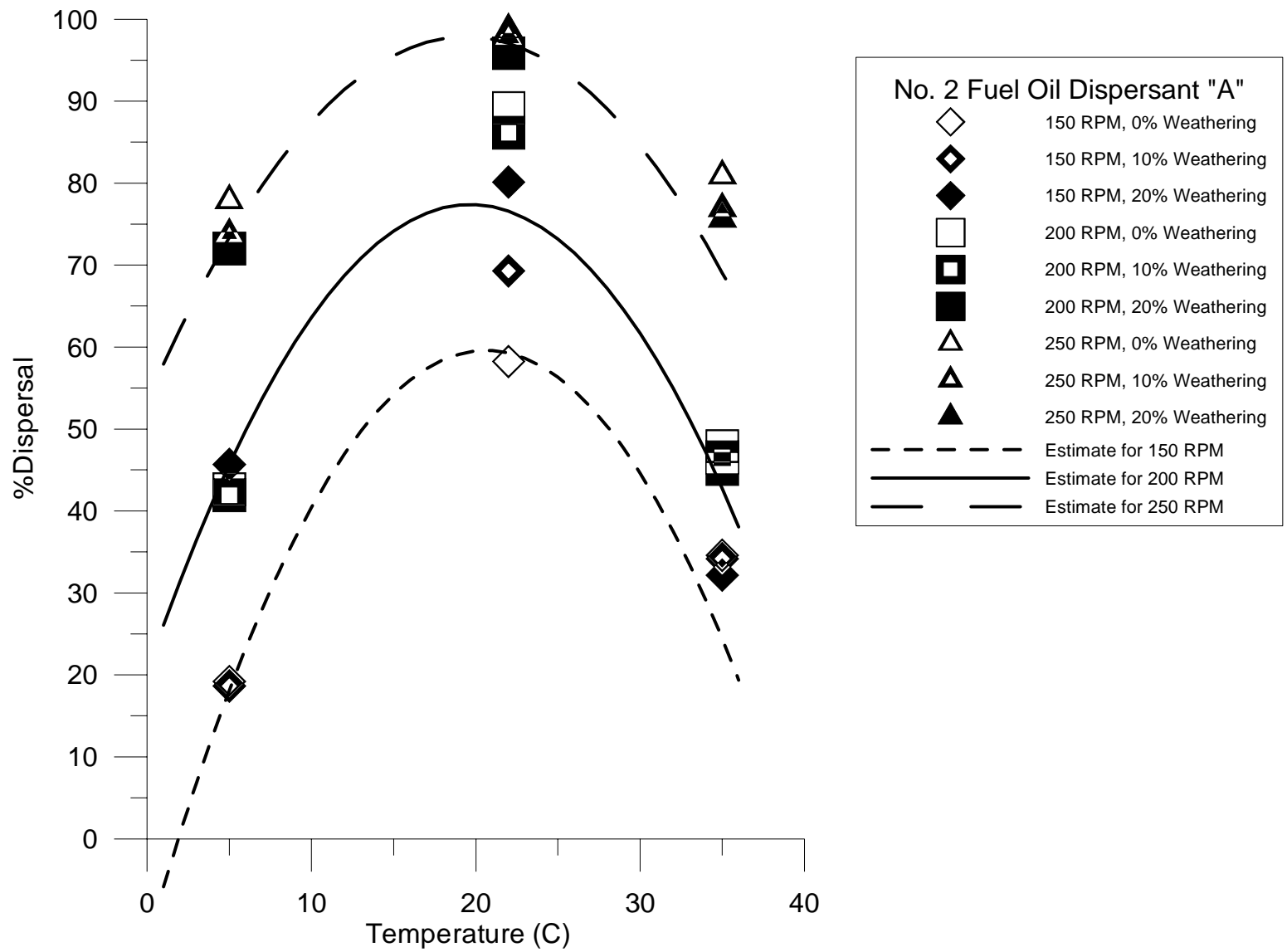


Figure 32 Comparison of regression equations (curves) against measured No. 2 Fuel Oil/Dispersant "A" efficiency.

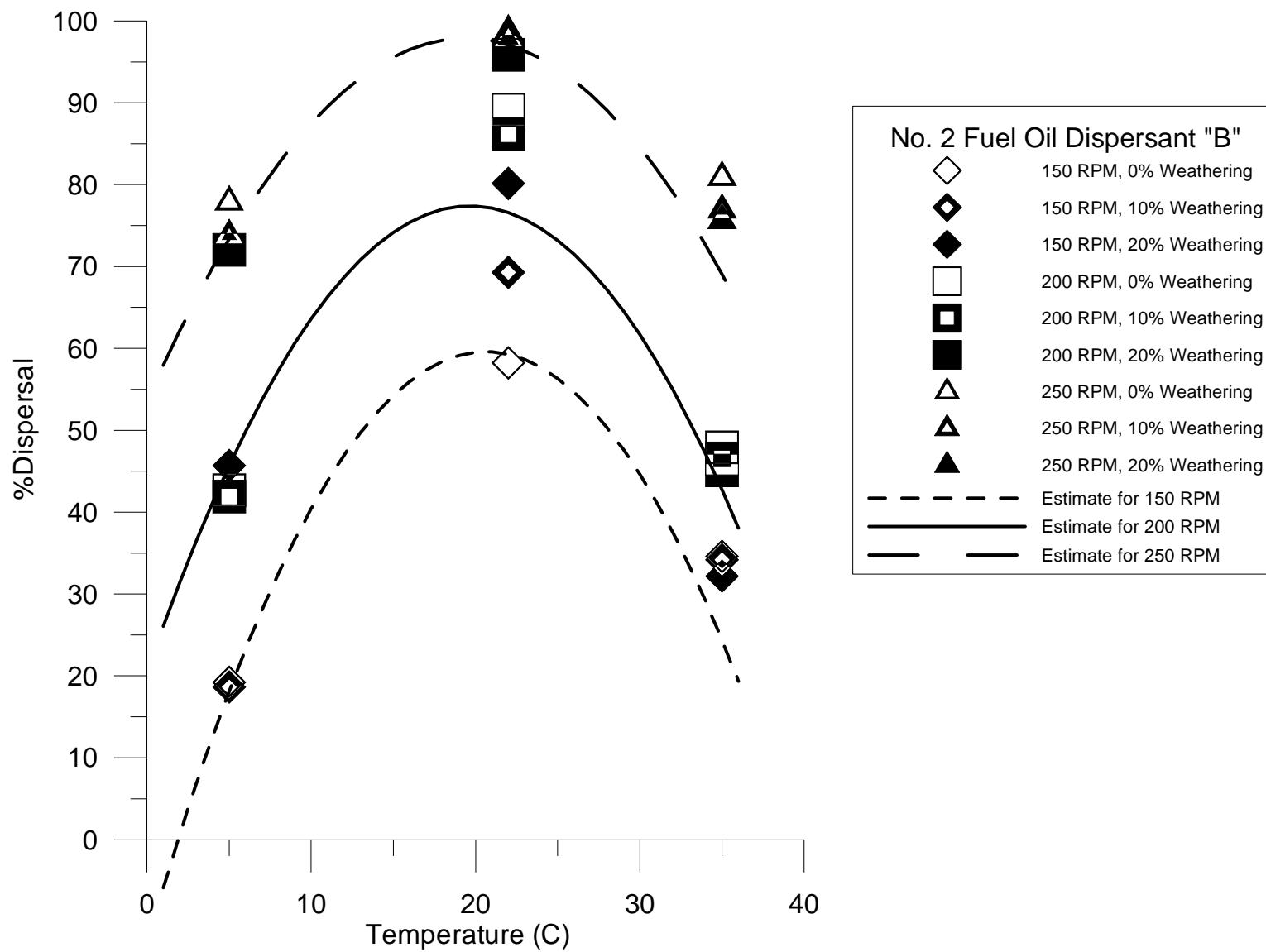


Figure 33 Comparison of regression equations (curves) against measured No. 2 Fuel Oil/Dispersant “B” efficiency.

Appendix: Wang et al. (2003) Physical Properties and Chemical Composition of Alaska North Slope Crude Oil

- 1 Origin:** Alaska, U.S.A (the oil was drawn as a line sample off the TAPS pipeline where it spurs off to the Petrostar Refinery in Valdez on March 19, 2002)
Synonyms: ANS
Appearance: Brown-black, light, little odour, fine black particulates dispersed through-out liquid.

Values are reported for the **fresh oil** and for artificially weathered fractions of **10.0%**, **22.5%** and **30.5%** loss by weight. The notations “(n=2),” “(n=2),” “(n=4),” etc indicate the number of replicates.

2 API Gravity

30.89 (*calc*)

3 Equation for Predicting Evaporation

$$\%Ev = (2.86 + 0.045 T) \ln t$$

Where: %Ev = weight percent evaporated; T = surface temperature (°C); t = time (minutes)

4 Sulphur Content

Weathering (weight %)	Sulphur (weight %)	
0	1.11	(n=3)
10.0	1.20	(n=3)
22.5	1.38	(n=3)
30.5	1.50	(n=3)

5 Water Content

Weathering (weight %)	Water (volume %)	
0	< 0.1	(n=3)
10.0	< 0.1	(n=3)
22.5	< 0.1	(n=3)
30.5	< 0.1	(n=3)

6 Flash Point

Weathering (weight %)	Flash Point (°C)	
0	<-8	(n=3)
10.0	19	(n=3)
22.5	75	(n=3)
30.5	115	(n=3)

7 Density

Weathering (weight %)	Temperature (°C)	Density (g/mL)	
0	0	0.8777	(n=3)
	15	0.8663	(n=3)
10.0	0	0.9054	(n=3)
	15	0.8940	(n=3)
22.5	0	0.9303	(n=3)
	15	0.9189	(n=3)
30.5	0	0.9457	(n=3)
	15	0.9340	(n=3)

8 Pour Point

Weathering (weight %)	Pour Point (°C)	
0	-32	(n=2)
10.0	-20	(n=2)
22.5	-9	(n=2)
30.5	-6	(n=2)

9 Dynamic Viscosity

Weathering (weight %)	Temperature (°C)	Viscosity (cP)	
0	0	23.2	(n=3)
	15	11.5	(n=3)
10.0	0	76.7	(n=3)
	15	31.8	(n=3)
22.5	0	614	(n=2)
	15	152	(n=3)
30.5	0	4230	(n=2)
	15	624.7	(n=2)

10 Chemical Dispersibility

Weathering (weight %)	Chemical Dispersibility using Corexit 9500 (%)	
0	47	(n=6)
10.0	45	(n=6)
22.5	34	(n=6)
30.5	15	(n=6)

11 Adhesion

Weathering (weight %)	Adhesion (g/m ²)	
0	20	(n=4)
10.0	35	(n=4)
22.5	38	(n=4)
30.5	40	(n=4)

12 Surface and Interfacial Tensions

12.1 Surface Tension (Oil/Air Interfacial Tension)

Weathering (weight %)	Temperature (°C)	Surface Tension (mN/m)	
0	0	27.3	(n=3)
	15	26.4	(n=3)
10.0	0	29.8	(n=3)
	15	28.4	(n=3)
22.5	0	31.2	(n=3)
	15	30.4	(n=3)
30.5	0	33.1	(n=3)
	15	31.8	(n=3)

12.2 Oil/Brine (33‰) Interfacial Tension

Weathering (weight %)	Temperature (°C)	Surface Tension (mN/m)	
0	0	22.5	(n=3)
	15	20.2	(n=3)
10.0	0	25.3	(n=3)
	15	23.1	(n=3)
22.5	0	26.8	(n=3)
	15	24.2	(n=3)
30.5	0	30.1	(n=3)
	15	25.6	(n=3)

12.3 Oil/Fresh Water Interfacial Tension

Weathering (weight %)	Temperature (°C)	Surface Tension (mN/m)	
0	0	26.7	(n=3)
	15	23.6	(n=3)
10.0	0	28.1	(n=3)
	15	25.5	(n=3)
22.5	0	30.8	(n=3)
	15	27.7	(n=3)
30.5	0	33.2	(n=3)
	15	30.2	(n=3)

13 Emulsion Formation

Weathering (weight %)	Visual Stability	Complex Modulus (Pa)	Emulsion Water Content (%)
0	Unstable		
10.0	Unstable		
22.5	Unstable		
30.5	Mesostable	155	72.9

14 Boiling Point Distribution

Boiling Point (°C)	Cumulative Weight Fraction (%)			
	0% weathered	10.0% weathered	22.5% weathered	30.5% weathered
40	2.5	0.1		
60	3.9	0.5		
80	6.5	1.4		
100	10.0	3.6		
120	13.4	6.6	0.1	
140	16.6	9.8	0.6	
160	19.8	13.1	2.0	
180	22.6	16.3	4.4	
200	25.2	19.2	7.3	0.5
250	32.6	27.4	16.6	7.5
300	40.7	36.4	27.0	18.7
350	49.5	46.1	38.2	31.1
400	57.7	55.3	48.7	42.8
450	66.0	64.5	59.3	54.5
500	72.8	72.1	68.2	64.2
550	79.0	79.0	76.0	72.8
600	84.1	84.7	82.6	79.9
650	88.4	89.5	88.0	85.8

15 Hydrocarbon Groups

Component	Concentration (weight %)			
	0% weathered	10.0% weathered	22.5% weathered	30.5% weathered
Saturates	75.0	72.1	69.2	64.8
Aromatics	15.0	16.0	16.5	18.5
Resins	6.1	7.4	8.9	10.3
Asphaltenes	4.0	4.4	5.4	6.4
Waxes	2.6	2.9	3.3	3.6

16 Volatile Organic Compounds

Component	Concentration ($\mu\text{g/g}$ oil)	
	0% weathered	30.5% weathered
Benzene	2866	0
Toluene	5928	0
Ethylbenzene	1319	0
Xylenes [†]	6187	0
C ₃ -Benzenes [‡]	5620	30
Total BTEX	16300	0
Total BTEX and C ₃ - Benzenes [‡]	21920	30

[†]“Xylenes” include *o*-, *m*-, and *p*-xylene isomers.

[‡]“C₃-Benzenes” include eight isomers.

17 *n*-Alkane Distribution

<i>n</i> -Alkane Component	Concentration (mg/g oil)	
	0% weathered	30.5% weathered
<i>n</i> -C8	5.55	
<i>n</i> -C9	4.29	
<i>n</i> -C10	4.13	
<i>n</i> -C11	3.98	0.73
<i>n</i> -C12	3.71	2.51
<i>n</i> -C13	3.57	3.80
<i>n</i> -C14	3.42	4.58
<i>n</i> -C15	3.28	4.34
<i>n</i> -C16	3.15	4.05
<i>n</i> -C17	3.06	4.00
Pristane	1.89	2.41
<i>n</i> -C18	2.68	3.46
Phytane	1.41	1.80
<i>n</i> -C19	2.32	2.93
<i>n</i> -C20	2.11	2.71
<i>n</i> -C21	1.96	2.50
<i>n</i> -C22	1.90	2.45
<i>n</i> -C23	1.79	2.34
<i>n</i> -C24	1.65	2.16
<i>n</i> -C25	1.47	1.94
<i>n</i> -C26	1.27	1.73
<i>n</i> -C27	0.97	1.28
<i>n</i> -C28	0.78	1.03
<i>n</i> -C29	0.70	0.98
<i>n</i> -C30	0.56	0.69
<i>n</i> -C31	0.44	0.60
<i>n</i> -C32	0.31	0.43
<i>n</i> -C33	0.27	0.33
<i>n</i> -C34	0.24	0.31
<i>n</i> -C35	0.22	0.25
<i>n</i> -C36	0.11	0.14
<i>n</i> -C37	0.09	0.13
<i>n</i> -C38	0.07	0.10
<i>n</i> -C39	0.05	0.07
<i>n</i> -C40	0.03	0.06
<i>n</i> -C41	0.02	0.04
TOTAL	63.4	56.9
C17/PRISTANE	1.62	1.66
C18/PHYTANE	1.9	1.92
PRISTANE/PHYTANE	1.35	1.34
CPI	0.9	1.0

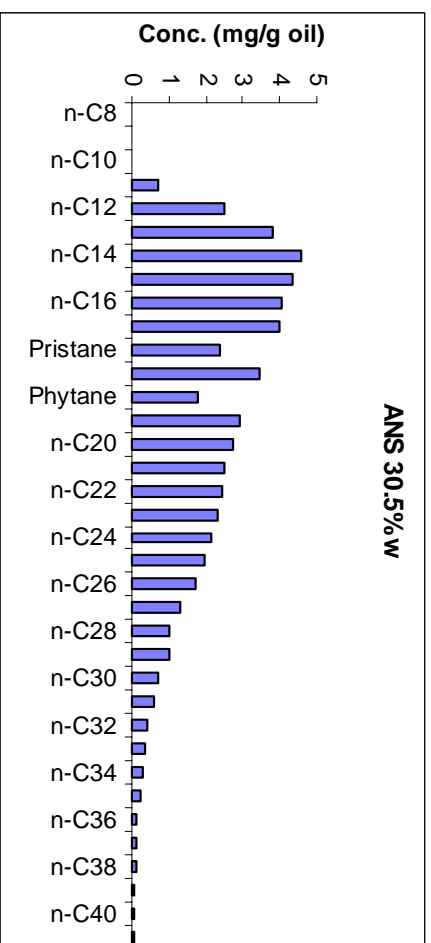
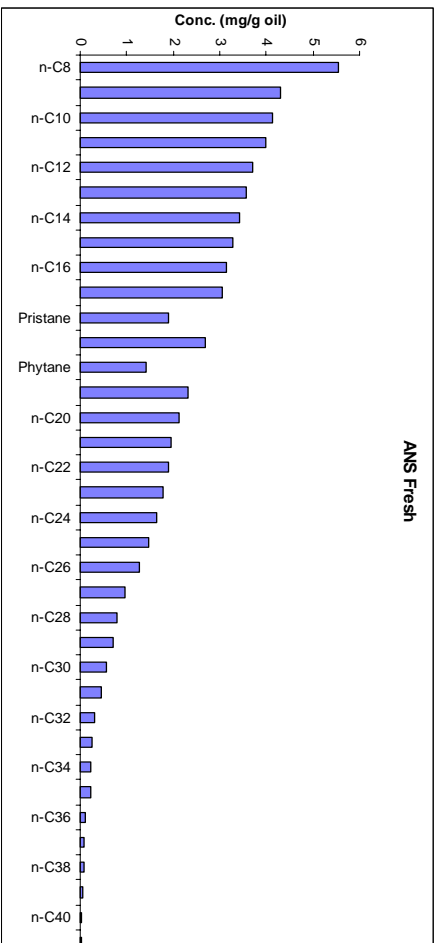


Figure 1 *n*-Alkane Distribution for Alaska North Slope crude oil (mg/g oil)

18 PAH Distribution

		Concentration (µg/g oil)	
Alkylated PAH		0% weathered	30.5% weathered
Naphthalene			
	C0-N	261	167
	C1-N	1015	1288
	C2-N	1800	2716
	C3-N	1702	2575
	C4-N	815	1174
	Sum	5594	7919
Phenanthrene			
	C0-P	209	295
	C1-P	666	932
	C2-P	710	988
	C3-P	486	707
	C4-P	296	432
	Sum	2368	3354
Dibenzothiophene			
	C0-D	122	174
	C1-D	225	319
	C2-D	318	456
	C3-D	265	362
	Sum	931	1312
Fluorene			
	C0-F	142	197
	C1-F	328	449
	C2-F	447	647
	C3-F	379	525
	Sum	1295	1819
Chrysene			
	C0-C	48	68
	C1-C	74	107
	C2-C	99	141
	C3-C	84	115
	Sum	306	430
TOTAL		10493	14834
2-m-N/1-m-N		1.49	1.41
(3+2-m/phen)/(4-/9-+1m-phen)		0.76	0.76
4-m:2/3m:1-m-DBT		1 : 0.65 : 0.34	1 : 0.65 : 0.34
Other PAHs			
	Biphenyl	134.71	176.9
	Acenaphthylene	12.03	18.43
	Acenaphthene	13.03	20.02
	Anthracene	2.88	4.55
	Fluoranthene	2.88	3.81
	Pyrene	8.40	11.92
	Benz(a)anthracene	4.64	8.11
	Benzo(b)fluoranthene	5.14	7.49
	Benzo(k)fluoranthene	0.50	0.70
	Benzo(e)pyrene	10.28	14.74
	Benzo(a)pyrene	2.26	3.69
	Perylene	3.01	4.42
	Indeno(1,2,3cd)pyrene	0.13	0.25
	Dibenz(a,h)anthracene	0.63	1.02
	Benzo(ghi)perylene	3.13	4.91
TOTAL		204	281

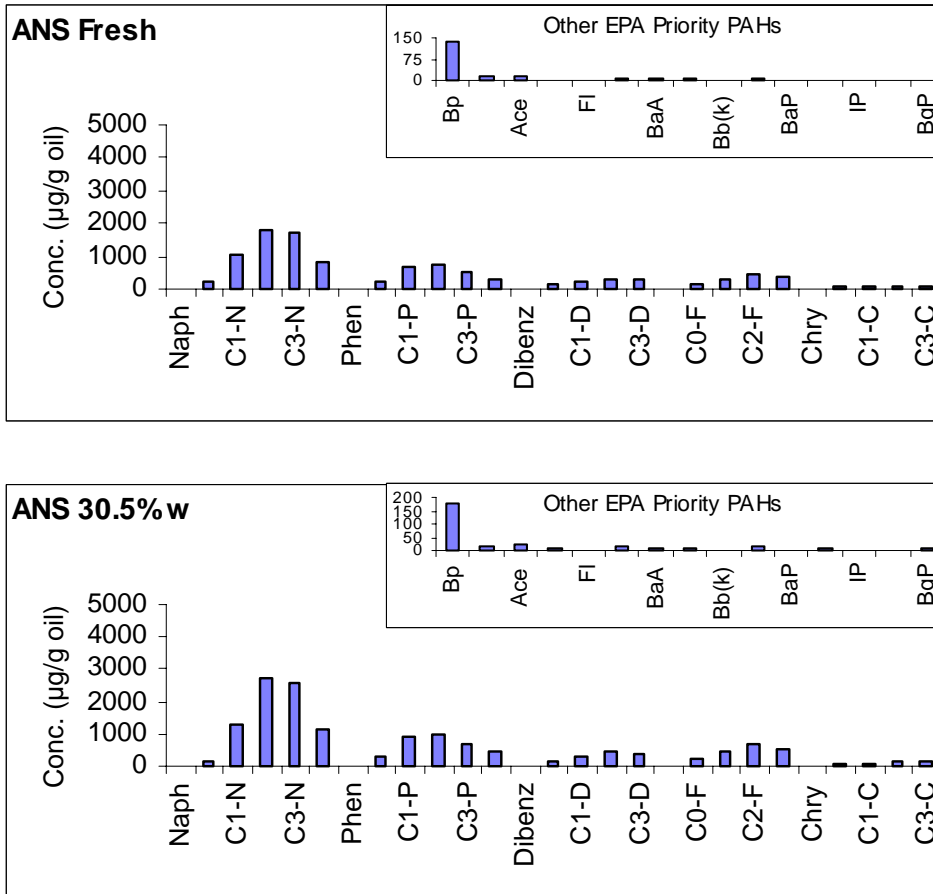


Figure 2 PAH Distribution for Alaska North Slope crude oil (µg/g oil)

19 Biomarker Concentrations

Biomarker	Concentration ($\mu\text{g/g oil}$)	
	0% weathered	30.5% weathered
C23	65.6	91.8
C24	40.8	57.8
C29	77.6	104.6
C30	116.6	161.1
C31(S)	46.9	64.1
C31(R)	33.0	46.1
C32(S)	34.2	46.5
C32(R)	21.6	30.9
C33(S)	21.6	31.0
C33(R)	13.3	19.3
C34(S)	15.1	21.0
C34(R)	8.6	12.4
Ts	20.9	31.8
Tm	28.5	43.0
C27 $\alpha\beta\beta$ steranes	73.6	103.2
C29 $\alpha\beta\beta$ steranes	84.2	113.8
TOTAL	702	978

Diagnostic Ratios

C23/C24	1.61	1.59
C23/C30	0.56	0.57
C24/C30	0.35	0.36
C29/C30	0.67	0.65
C31(S)/C31(R)	1.42	1.39
C32(S)/C32(R)	1.58	1.51
C33(S)/C33(R)	1.62	1.60
C34(S)/C34(R)	1.76	1.70
Ts/Tm	0.73	0.74
C27 $\alpha\beta\beta$ /C29 $\alpha\beta\beta$	0.87	0.91

Appendix: Wang et al, (2003) Physical Properties and Chemical Composition of South Louisiana

- 1 **Origin:** Baton Rouge, Louisiana, U.S.A. (Exxon-Mobil)
Synonyms: Louisiana

Values are reported for the **fresh oil** and for artificially weathered fractions of **10.9%**, **19.7%** and **27.7%** loss by weight. The notations “(n=2),” “(n=2),” “(n=4),” etc indicate the number of replicates.

2 **API Gravity**

32.72 (*calc*)

3 **Equation for Predicting Evaporation**

$$\%Ev = (2.74 + 0.045 T) \ln t$$

Where: %Ev = weight percent evaporated; *T* = surface temperature (°C); *t* = time (minutes)

4 **Sulphur Content**

Weathering (weight %)	Sulphur (weight %)	
0	0.49	(n=3)
10.9	0.71	(n=3)
19.7	0.79	(n=3)
27.7	0.88	(n=3)

5 **Water Content**

Weathering (weight %)	Water (volume %)	
0	<0.1	(n=3)
10.9	<0.1	(n=3)
19.7	<0.1	(n=3)
27.7	<0.1	(n=3)

6 Flash Point

Weathering (weight %)	Flash Point (°C)	
0	<-10	(n=2)
10.9	42.3	(n=3)
19.7	80.7	(n=3)
27.7	>110	(n=2)

7 Density

Weathering (weight %)	Temperature (°C)	Density (g/mL)	
0	0	0.8668	(n=3)
	15	0.8562	(n=3)
10.9	0	0.8888	(n=3)
	15	0.8770	(n=3)
19.7	0	0.9025	(n=3)
	15	0.8906	(n=3)
27.7	0	0.9135	(n=3)
	15	0.9018	(n=3)

8 Pour Point

Weathering (weight %)	Pour Point (°C)	
0	-41	(n=2)
10.9	-19	(n=2)
19.7	-14	(n=1)
27.7	-11	(n=2)

9 Dynamic Viscosity

Weathering (weight %)	Temperature (°C)	Viscosity (cP)	
0	0	18.5	(n=3)
	15	10.1	(n=3)
10.9	0	54.8	(n=3)
	15	23.7	(n=3)
19.7	0	217.3	(n=3)
	15	48.9	(n=2)
27.7	0	515.9	(n=3)
	15	141.0	(n=3)

10 Chemical Dispersibility

Weathering (weight %)	Chemical Dispersibility using Corexit 9500 (%)	
0	26.5	(n=6)
10.9	23.5	(n=6)
19.7	15.8	(n=6)
27.7	10.3	(n=6)

11 Adhesion

Weathering (weight %)	Adhesion (g/m ²)	
0	24	(n=4)
10.9	34	(n=4)
19.7	50	(n=5)
27.7	28	(n=4)

12 Surface and Interfacial Tensions

12.1 Surface Tension (Oil/Air Interfacial Tension)

Weathering (weight %)	Temperature (°C)	Surface Tension (mN/m)	
0	0	28.3	(n=3)
	15	26.1	(n=3)
10.9	0	29.3	(n=3)
	15	28.1	(n=3)
19.7	0	30.4	(n=3)
	15	29.4	(n=3)
27.7	0	31.1	(n=3)
	15	29.8	(n=3)

12.2 Oil/Brine (33‰) Interfacial Tension

Weathering (weight %)	Temperature (°C)	Surface Tension (mN/m)	
0	0	20.9	(n=2)
	15	16.8	(n=3)
10.9	0	22.0	(n=3)
	15	19.4	(n=2)
19.7	0	22.0	(n=3)
	15	22.2	(n=2)
27.7	0	20.6	(n=4)
	15	18.4	(n=3)

12.3 Oil/Fresh Water Interfacial Tension

Weathering (weight %)	Temperature (°C)	Surface Tension (mN/m)	
0	0	20.8	(n=3)
	15	15.5	(n=2)
10.9	0	25.2	(n=3)
	15	15.8	(n=3)
19.7	0	25.3	(n=3)
	15	22.3	(n=3)
27.7	0	24.7	(n=3)
	15	21.9	(n=3)

13 Emulsion Formation

Weathering (weight %)	Visual Stability	Complex Modulus (Pa)	Emulsion Water Content (%)
0	Unstable		
10.9	Unstable		
19.7	Unstable		
27.7	Unstable		

14 Boiling Point Distribution

Boiling Point (°C)	Cumulative Weight Fraction (%)			
	0% weathered	10.9% weathered	19.7% weathered	27.7% weathered
40	1.2			
60	1.6			
80	2.1			
100	5.6	0.9		
120	8.2	2.4	0.1	
140	11.1	4.8	0.4	
160	14.1	7.8	1.6	0.1
180	17.5	11.4	4.0	0.3
200	20.6	14.9	7.2	1.4
250	29.8	25.2	18.1	10.6
300	39.9	36.6	30.6	24.1
350	49.7	47.7	42.8	37.5
400	58.1	57.0	53.1	49.0
450	65.8	65.7	62.7	59.6
500	72.0	72.7	70.4	68.2
550	77.1	78.5	76.7	75.2
600	80.9	82.8	81.5	80.5
650	83.8	86.0	85.0	84.5

15 Hydrocarbon Groups

Component	Concentration (%)			
	0% weathered	10.9% weathered	19.7% weathered	27.7% weathered
Saturates	80.8	80.4	78.4	77.3
Aromatics	12.6	12.3	12.5	13.3
Resins	5.9	6.4	8.0	8.0
Asphaltenes	0.8	0.9	1.1	1.5
Waxes	1.7	1.8	2.0	2.2

16 Volatile Organic Compounds

Component	Concentration (µg/g oil)	
	0% weathered	27.7% weathered
Benzene	1598	0
Toluene	3552	10
Ethylbenzene	891	0
Xylenes [†]	6164	2
C ₃ -Benzenes [‡]	6680	190
Total BTEX	12210	12
Total BTEX and C ₃ -Benzenes [‡]	18890	202

[†]“Xylenes” include *o*-, *m*-, and *p*-xylene isomers.

[‡]“C₃-Benzenes” include eight isomers.

17 *n*-Alkane Distribution

<i>n</i> -Alkane Component	Concentration (mg/g oil)	
	0% weathered	27.7% weathered
<i>n</i> -C8	4.33	
<i>n</i> -C9	4.12	
<i>n</i> -C10	4.12	0.21
<i>n</i> -C11	4.56	1.81
<i>n</i> -C12	4.25	3.81
<i>n</i> -C13	4.14	4.94
<i>n</i> -C14	3.81	5.19
<i>n</i> -C15	3.88	5.29
<i>n</i> -C16	3.48	4.75
<i>n</i> -C17	3.05	4.13
Pristane	2.10	2.76
<i>n</i> -C18	2.24	3.11
Phytane	1.35	1.84
<i>n</i> -C19	2.00	2.61
<i>n</i> -C20	1.70	2.27
<i>n</i> -C21	1.55	2.11
<i>n</i> -C22	1.33	1.81
<i>n</i> -C23	1.13	1.58
<i>n</i> -C24	1.03	1.44
<i>n</i> -C25	0.92	1.28
<i>n</i> -C26	0.72	1.08
<i>n</i> -C27	0.54	0.78
<i>n</i> -C28	0.49	0.70
<i>n</i> -C29	0.42	0.62
<i>n</i> -C30	0.38	0.54
<i>n</i> -C31	0.31	0.46
<i>n</i> -C32	0.23	0.34
<i>n</i> -C33	0.18	0.27
<i>n</i> -C34	0.16	0.24
<i>n</i> -C35	0.15	0.20
<i>n</i> -C36	0.08	0.12
<i>n</i> -C37	0.07	0.10
<i>n</i> -C38	0.05	0.08
<i>n</i> -C39	0.04	0.07
<i>n</i> -C40	0.03	0.05
<i>n</i> -C41	0.02	0.04
TOTAL	59.0	56.7
C17/PRISTANE	1.45	1.50
C18/PHYTANE	1.65	1.68
PRISTANE/PHYTANE	1.55	1.49
CPI	0.95	1.02

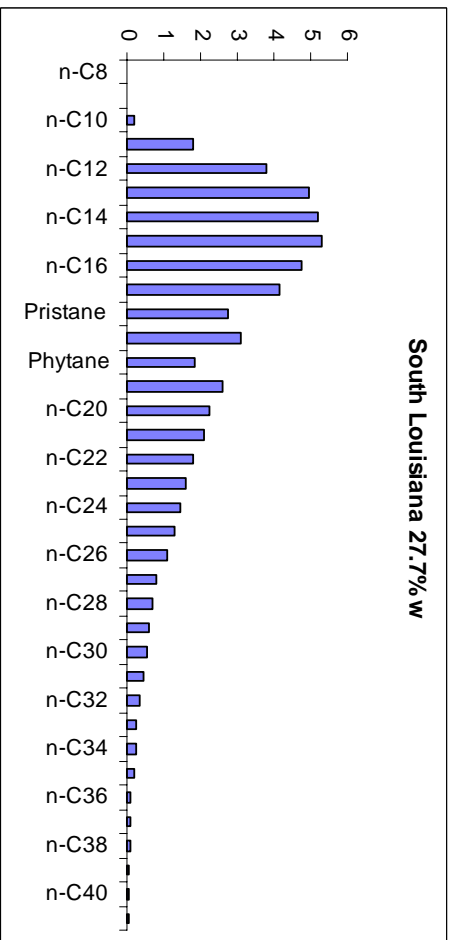
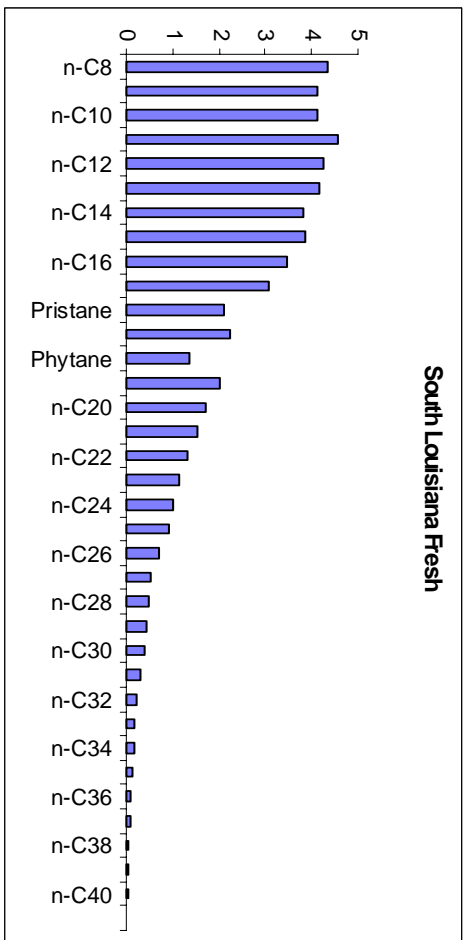


Figure 1 *n*-Alkane Distribution for South Louisiana Crude Oil (mg/g oil)

18 PAH Distribution

Alkylated PAH	Concentration (µg/g oil)	
	0% weathered	27.7% weathered
Naphthalene		
C0-N	248.6	164.1
C1-N	952.7	1058.9
C2-N	1500.1	1965.6
C3-N	1765.7	2403.6
C4-N	886.3	1222.3
Sum	5353	6815
Phenanthrene		
C0-P	134.4	188.3
C1-P	569.8	777.8
C2-P	654.6	887.1
C3-P	427.4	574.6
C4-P	251.8	349.6
Sum	2038	2777
Dibenzothiophene		
C0-D	40.0	55.4
C1-D	125.7	172.4
C2-D	237.4	323.1
C3-D	205.5	272.6
Sum	609	823
Fluorene		
C0-F	67.3	94.8
C1-F	181.7	253.2
C2-F	291.4	396.4
C3-F	246.0	354.1
Sum	804	1098
Chrysene		
C0-C	23.0	30.4
C1-C	58.8	80.1
C2-C	81.6	108.4
C3-C	69.1	90.7
Sum	233	310
TOTAL	9037	11823
2-m-N/1-m-N	1.63	1.59
(3+2-m/phen)/(4-/9-+1m-phen)	1.00	1.01
4-m:2/3m:1-m-DBT	1:0.62:0.31	1:0.61:0.31
Other PAHs		
Biphenyl	94.32	120.60
Acenaphthylene	8.15	10.70
Acenaphthene	17.90	24.27
Anthracene	2.47	3.61
Fluoranthene	3.70	5.10
Pyrene	8.64	11.33
Benzo(a)anthracene	5.19	6.35
Benzo(b)fluoranthene	2.10	3.73
Benzo(k)fluoranthene	0.37	1.24
Benzo(e)pyrene	4.07	5.97
Benzo(a)pyrene	0.49	0.62
Perylene	30.37	38.95
Indeno(1,2,3cd)pyrene	0.50	1.12
Dibenz(a,h)anthracene	0.86	1.12
Benzo(ghi)perylene	1.23	1.99
TOTAL	180	237

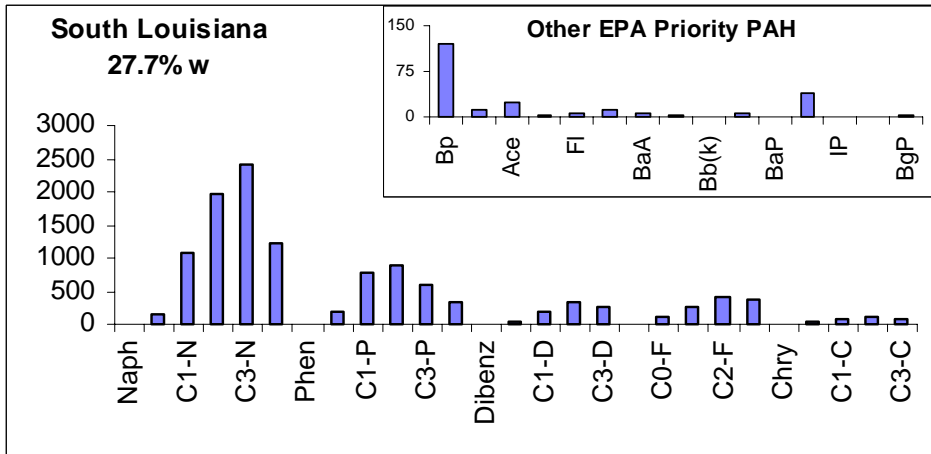
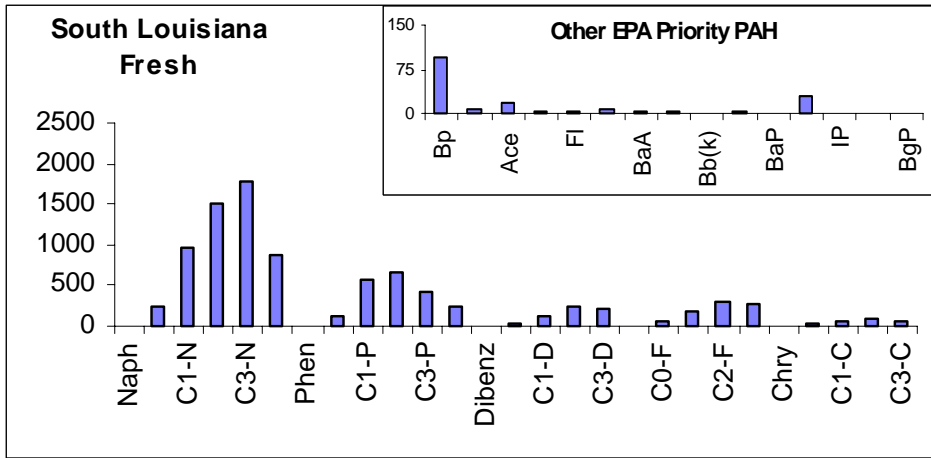


Figure 2 PAH Distribution for South Louisiana crude oil (µg/g oil)

19 Biomarker Concentrations

Biomarker	Concentration ($\mu\text{g/g oil}$)	
	0% weathered	27.7% weathered
C23	16.9	22.7
C24	11.2	14.7
C29	59.9	75.9
C30	81.5	105.6
C31(S)	31.0	40.2
C31(R)	27.5	35.7
C32(S)	20.1	25.1
C32(R)	13.6	17.4
C33(S)	12.2	15.4
C33(R)	8.8	10.5
C34(S)	6.1	7.3
C34(R)	4.4	5.2
Ts	19.0	24.3
Tm	23.1	30.3
C27 $\alpha\beta\beta$ steranes	65.0	85.8
C29 $\alpha\beta\beta$ steranes	72.8	94.3
TOTAL	473	610

Diagnostic Ratios		
C23/C24	1.50	1.54
C23/C30	0.21	0.21
C24/C30	0.14	0.14
C29/C30	0.73	0.72
C31(S)/C31(R)	1.13	1.13
C32(S)/C32(R)	1.48	1.44
C33(S)/C33(R)	1.39	1.46
C34(S)/C34(R)	1.37	1.41
Ts/Tm	0.82	0.80
C27 $\alpha\beta\beta$ /C29 $\alpha\beta\beta$	0.89	0.91

Appendix: Wang et al. (2003) Physical Properties and Chemical Composition of Fuel Oil No. 2/Diesel

- 1 Origin:** Local Retailer, Ontario, Canada (Stinsons' Gas)
Synonyms: "Summer" Diesel, Fuel Oil No. 2
Appearance: Golden-coloured, light, characteristic "fuel" odour.

Values are reported for the **fresh oil** and for artificially weathered fractions of **7.2%**, **14.2%** and **22.0%** loss by weight. The notations "(n=2)," "(n=2)," "(n=4)," etc indicate the number of replicates.

2 API Gravity

37.52 (*calc*)

3 Equation for Predicting Evaporation

$$\%Ev = (0.02 + 0.013 T) \sqrt{t}$$

Where: %Ev = weight percent evaporated; *T* = surface temperature (°C); *t* = time (minutes)

4 Sulphur Content

Weathering (weight %)	Sulphur (weight %)	
0	0.09	(n=3)
7.2	0.10	(n=3)
14.2	0.10	(n=3)
22.0	0.10	(n=3)

5 Water Content

Weathering (weight %)	Water (volume %)	
0	<0.1	(n=3)
7.2	<0.1	(n=3)
14.2	<0.1	(n=3)
22.0	<0.1	(n=3)

6 Flash Point

Weathering (weight %)	Flash Point (°C)	
0	54	(n=2)
7.2	65	(n=2)
14.2	76	(n=2)
22.0	85	(n=2)

7 Density

Weathering (weight %)	Temperature (°C)	Density (g/mL)	
0	0	0.8423	(n=3)
	15	0.8310	(n=3)
7.2	0	0.8468	(n=3)
	15	0.8350	(n=3)
14.2	0	0.8493	(n=3)
	15	0.8383	(n=3)
22.0	0	0.8524	(n=3)
	15	0.8416	(n=3)

8 Pour Point

Weathering (weight %)	Pour Point (°C)	
0	-50	(n=2)
7.2	-49	(n=2)
14.2	-43	(n=2)
22.0	-41	(n=2)

9 Dynamic Viscosity

Weathering (weight %)	Temperature (°C)	Viscosity (cP)	
0	0	4.08	(n=3)
	15	2.76	(n=3)
7.2	0	4.55	(n=3)
	15	3.27	(n=3)
14.2	0	5.16	(n=3)
	15	3.42	(n=2)
22.0	0	5.59	(n=3)
	15	4.18	(n=2)

10 Chemical Dispersibility

Weathering (weight %)	Chemical Dispersibility using Corexit 9500 (%)	
0	72	(n=6)
7.2	71	(n=6)
14.2	64	(n=6)
22.0	66	(n=6)

11 Adhesion

Weathering (weight %)	Adhesion (g/m ²)	
0	2	(n=4)
7.2	12	(n=4)
14.2	13	(n=3)
22.0	8	(n=4)

12 Surface and Interfacial Tensions

12.1 Surface Tension (Oil/Air Interfacial Tension)

Weathering (weight %)	Temperature (°C)	Surface Tension (mN/m)	
0	0	28.7	(n=3)
	15	27.5	(n=3)
7.2	0	28.8	(n=3)
	15	27.7	(n=3)
14.2	0	28.6	(n=3)
	15	28.1	(n=3)
22.0	0	29.3	(n=3)
	15	28.3	(n=3)

12.2 Oil/Brine (33‰) Interfacial Tension

Weathering (weight %)	Temperature (°C)	Surface Tension (mN/m)	
0	0	21.5	(n=3)
	15	18.1	(n=8)
7.2	0	24.8	(n=3)
	15	19.5	(n=3)
14.2	0	26.6	(n=2)
	15	20.7	(n=3)
22.0	0	28.5	(n=3)
	15	21.9	(n=3)

12.3 Oil/Fresh Water Interfacial Tension

Weathering (weight %)	Temperature (°C)	Surface Tension (mN/m)	
0	0	25.0	(n=3)
	15	21.6	(n=3)
7.2	0	28.1	(n=3)
	15	23.9	(n=3)
14.2	0	28.5	(n=3)
	15	24.3	(n=3)
22.0	0	29.1	(n=3)
	15	25.7	(n=2)

13 Emulsion Formation

Weathering (weight %)	Visual Stability	Complex Modulus (Pa)	Emulsion Water Content (%)
0	Unstable		
7.2	Unstable		
14.2	Unstable		
22.0	Unstable		

14 Boiling Point Distribution

Boiling Point (°C)	Cumulative Weight Fraction (%)			
	0% weathered	7.2% weathered	14.2% weathered	22.0% weathered
40				
60				
80	0.2	0.1		
100	0.5	0.1		
120	1.2	0.1		
140	2.8	0.7	0.1	
160	7.8	4.0	1.4	0.3
180	16.4	11.8	7.1	3.2
200	26.8	22.4	17.0	11.2
250	57.4	55.4	51.7	46.7
300	84.1	84.5	83.3	81.4
350	96.4	98.1	98.1	97.8
400	97.9	99.7	99.8	99.7
450	98.1	99.9		
500	98.2			
550	98.3			
600	98.4			
650	98.6			

15 Hydrocarbon Groups

Component	Concentration (weight %)			
	0% weathered	7.2% weathered	14.2% weathered	22.0% weathered
Saturates	88.2	86.1	86.1	85.6
Aromatics	10.2	11.9	11.7	11.4
Resins	1.7	2.0	2.2	3.0
Asphaltenes	0.0	0.0	0.0	0.0
Waxes	1.7	1.8	2.0	1.8

16 Volatile Organic Compounds

Component	Concentration ($\mu\text{g/g}$ oil)	
	0% weathered	22.0% weathered
Benzene	136	0
Toluene	1024	0
Ethylbenzene	619	0
Xylenes [†]	3774	7
C ₃ -Benzenes ^{††}	13780	2260
Total BTEX	5550	7
Total BTEX and C ₃ - Benzenes [‡]	19330	2267

[†]Note that the "Xylenes" include *o*-, *m*-, and *p*-xylene isomers.

^{††}Note that the "C₃-Benzenes" include eight isomers.

17 *n*-Alkane Distribution

<i>n</i> -Alkane Component	Concentration (mg/g oil)	
	0% weathered	22.0% weathered
<i>n</i> -C8	1.15	
<i>n</i> -C9	4.24	
<i>n</i> -C10	10.93	3.96
<i>n</i> -C11	13.43	11.79
<i>n</i> -C12	13.23	15.25
<i>n</i> -C13	13.02	16.51
<i>n</i> -C14	12.33	15.77
<i>n</i> -C15	11.98	15.58
<i>n</i> -C16	10.96	13.70
<i>n</i> -C17	9.22	11.37
Pristane	3.81	4.82
<i>n</i> -C18	6.72	8.20
Phytane	2.52	3.10
<i>n</i> -C19	4.72	5.88
<i>n</i> -C20	3.01	3.74
<i>n</i> -C21	1.70	2.11
<i>n</i> -C22	0.85	1.06
<i>n</i> -C23	0.41	0.52
<i>n</i> -C24	0.19	0.24
<i>n</i> -C25	0.09	0.11
<i>n</i> -C26	0.04	0.05
<i>n</i> -C27	0.02	0.03
<i>n</i> -C28	0.02	0.02
<i>n</i> -C29	0.01	0.01
<i>n</i> -C30	0.01	0.01
<i>n</i> -C31	0.01	0.01
<i>n</i> -C32		
<i>n</i> -C33		
<i>n</i> -C34		
<i>n</i> -C35		
<i>n</i> -C36		
<i>n</i> -C37		
<i>n</i> -C38		
<i>n</i> -C39		
<i>n</i> -C40		
<i>n</i> -C41		
TOTAL	124.6	133.8
C17/PRISTANE	1.58	1.52
C18/PHYTANE	1.61	1.58
PRISTANE/PHYTANE	1.25	1.23
CPI	0.99	1.03

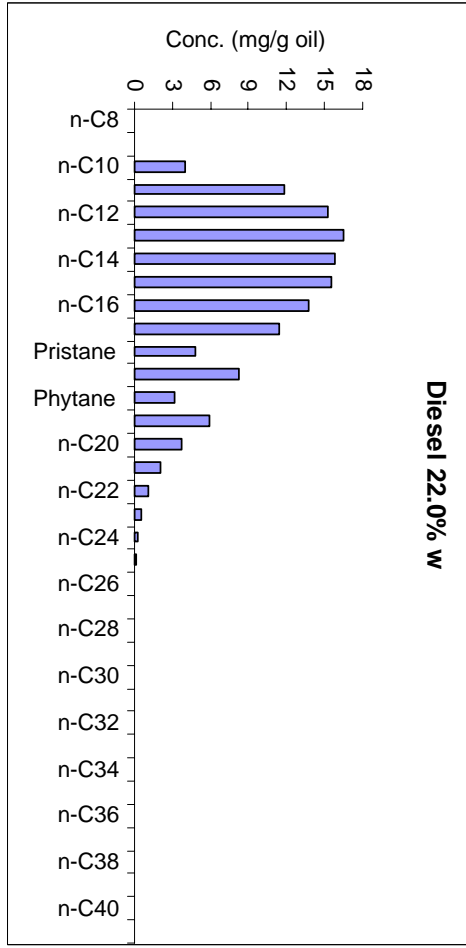
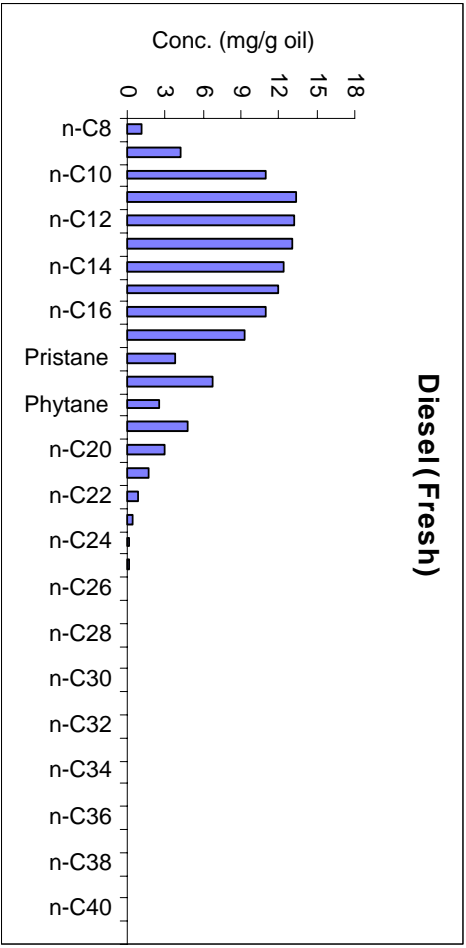


Figure 1 Alkane Distribution for Fuel Oil No. 2 (Diesel) (mg/g oil)

18 PAH Distribution

		Concentration (µg/g oil)	
Alkylated PAH		0% weathered	22.0% weathered
Naphthalene			
	C0-N	820	677
	C1-N	3664	3968
	C2-N	6927	8101
	C3-N	6636	8163
	C4-N	2805	3427
	Sum	20852	24337
Phenanthrene			
	C0-P	437	557
	C1-P	1000	1262
	C2-P	617	769
	C3-P	185	237
	C4-P	53	65
	Sum	2293	2890
Dibenzothiophene			
	C0-D	65	82
	C1-D	110	137
	C2-D	99	123
	C3-D	38	50
	Sum	312	392
Fluorene			
	C0-F	567	713
	C1-F	799	1025
	C2-F	756	961
	C3-F	360	458
	Sum	2481	3157
Chrysene			
	C0-C	0.02	0.03
	C1-C	0.03	0.04
	C2-C	0.04	0.04
	C3-C	0.00	0.00
	Sum	0.09	0.12
TOTAL		25938	30776
2-m-N/1-m-N		1.56	1.53
(3+2-m/phen)/(4-/9-+1m-phen)		1.50	1.52
4-m:2/3m:1-m-DBT		1 : 0.35 : 0.16	1 : 0.36 : 0.17
Other PAHs			
	Biphenyl	839.73	1072.40
	Acenaphthylene	34.87	42.29
	Acenaphthene	153.55	187.34
	Anthracene	13.08	14.09
	Fluoranthene	6.60	8.48
	Pyrene	30.88	38.84
	Benz(a)anthracene	0.25	0.28
	Benzo(b)fluoranthene	0.00	0.00
	Benzo(k)fluoranthene	0.00	0.00
	Benzo(e)pyrene	0.00	0.00
	Benzo(a)pyrene	0.00	0.00
	Perylene	0.00	0.00
	Indeno(1,2,3cd)pyrene	0.00	0.00
	Dibenz(a,h)anthracene	0.00	0.00
	Benzo(ghi)perylene	0.00	0.00
TOTAL		1080	1364

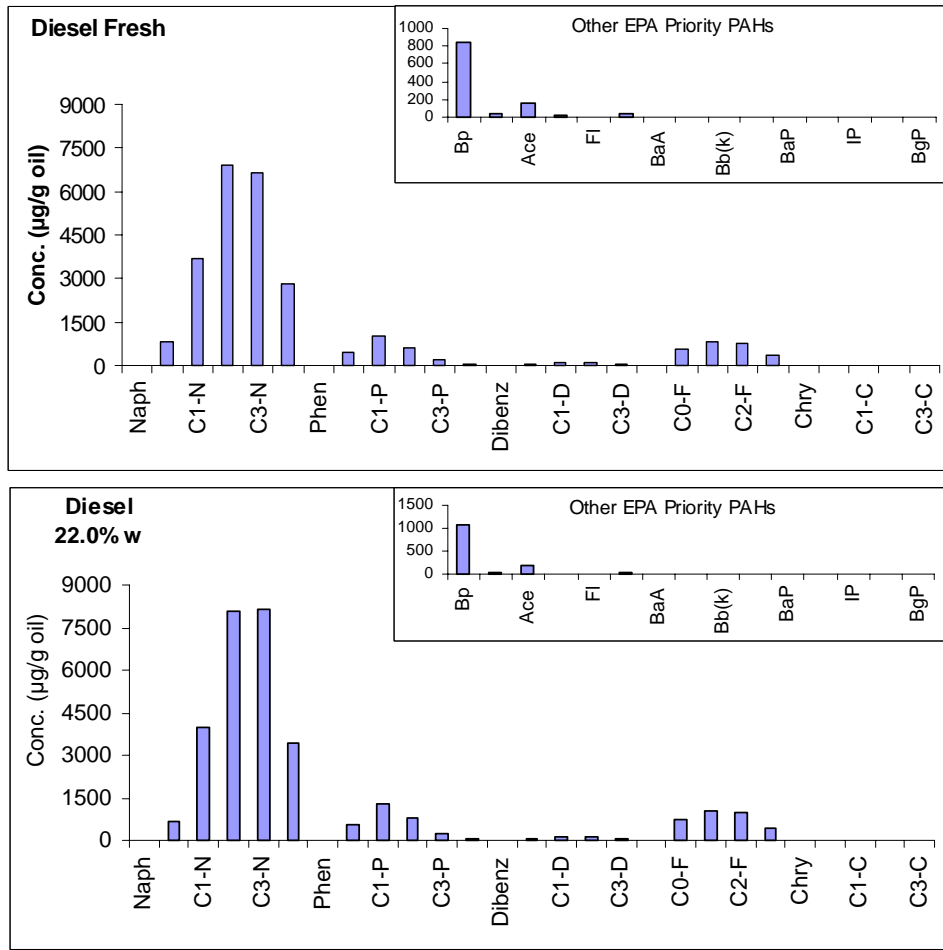


Figure 1 PAH Distribution for Fuel Oil No. 2 (Diesel) (µg/g oil)

19 Biomarker Concentrations

Biomarker	Concentration ($\mu\text{g/g oil}$)	
	0% weathered	22.0% weathered
C23	4.0	5.3
C24	1.4	1.8
C29		
C30		
C31(S)		
C31(R)		
C32(S)		
C32(R)		
C33(S)		
C33(R)		
C34(S)		
C34(R)		
Ts		
Tm		
C27 $\alpha\beta$ steranes		
C29 $\alpha\beta$ steranes		
TOTAL	5	7

Diagnostic Ratios		
C23/C24	3.0	2.9
C23/C30		
C24/C30		
C29/C30		
C31(S)/C31(R)		
C32(S)/C32(R)		
C33(S)/C33(R)		
C34(S)/C34(R)		
Ts/Tm		
C27 $\alpha\beta$ /C29 $\alpha\beta$		

Note: except for the C23 and C24 terpanes,
no other biomarkers were detected.